EUROPEAN Journal of Molecular Biotechnology

Has been issued since 2013.
ISSN 2310-6255. E-ISSN 2409-1332
2017. 5(1). Issued 2 times a year

EDITORIAL BOARD

Novochadov Valerii – Volgograd State University, Russian Federation (Editor in Chief)
Goncharova Nadezhda – Research Institute of Medical Primatology, Sochi, Russian Federation
Mosin Oleg – Moscow State University of Applied Biotechnology, Russian Federation
Garbuzova Victoriia – Sumy State University, Ukraine
Ignatov Ignat – Scientific Research Center of Medical Biophysics, Sofia, Bulgaria
Malcevschi Alessio – University of Parma, Italy
Nefedeva Elena – Volgograd State Technological University, Russian Federation
Kestutis Baltakys – Kaunas University of Technology, Lithuania
Tarantseva Klara – Penza State Technological University, Russian Federation
Venkappa S. Mantur – USM-KLE International Medical College, Karnatak, India

Journal is indexed by: **Chemical Abstracts Service** (USA), **CiteFactor** – Directory of International Reseach Journals (Canada), **Cross Ref** (UK), **EBSCOhost Electronic Journals Service** (USA), **Global Impact Factor** (Australia), **International Society of Universal Research in Sciences** (Pakistan), **Journal Index** (USA), **Electronic scientific library** (Russian Federation), O**pen Academic Journals Index** (Russian Federation), **Sherpa Romeo** (Spain), **ULRICH's WEB** (USA), **Universal Impact Factor** (Australia).

All manuscripts are peer reviewed by experts in the respective field. Authors of the manuscripts bear responsibility for their content, credibility and reliability.

Editorial board doesn't expect the manuscripts' authors to always agree with its opinion.

Postal Address: 1367/4, Stara Vajnorska str., Bratislava, Slovakia, Nove Mesto, 831 04

Website: http://ejournal8.com/
E-mail: aphr2010@mail.ru

Founder and Editor: Academic Publishing House Researcher s.r.o.

Release date 15.03.17.
Format 21 × 29,7/4.

Headset Georgia.

Order № 15.

© European Journal of Molecular Biotechnology, 2017

European Journal of Molecular Biotechnology

2017

Is. 1

European Journal of Molecular Biotechnology

2017

№ 1

EUROPEAN Journal of Molecular Biotechnology

Издается с 2013 г.
ISSN 2310-6255. E-ISSN 2409-1332
2016. № 4 (14). Выходит 4 раза в год.

РЕДАКЦИОННЫЙ СОВЕТ

Новочадов Валерий – Волгоградский государственный университет, Волгоград, Российская Федерация (Гл. редактор)
Гончарова Надежда – Научно-исследовательский институт медицинской приматологии РАМН, Сочи, Российская Федерация
Мосин Олег – Московский государственный университет прикладной биотехнологии, Москва, Российская Федерация
Венкаппа С. Мантур – Международный медицинский колледж, Карнатака, Индия
Гарбузова Виктория – Сумский государственный университет, Сумы, Украина
Игнатов Игнат – Научно-исследовательский центр медицинской биофизики, София, Болгария
Кястутис Балтакис – Каунасский технологический университет, Литва
Малкевсчи Алессио – Университет города Парма. Парма, Италия
Нефедьева Елена – Волгоградский государственный технический университет, Волгоград, Российская Федерация
Таранцева Клара – Пензенский государственный технологический университет, Пенза, Российская Федерация

Журнал зарегистрирован Федеральной службой по надзору в сфере массовых коммуникаций, связи и охраны культурного наследия (Российская Федерация). Свидетельство о регистрации средства массовой информации ПИ № ФС77-55114 от 26.08.2013 г.

Журнал индексируется в: **Chemical Abstracts Service** (США), **CiteFactor** – Directory of International Reseach Journals (Канада), **Cross Ref** (Великобритания), **EBSCOhost Electronic Journals Service** (США), **Global Impact Factor** (Австралия), **International Society of Universal Research in Sciences** (Пакистан), **Journal Index** (США), **Научная электронная библиотека** (Россия), **Open Academic Journals Index** (Россия), **Sherpa Romeo** (Испания), **ULRICH's WEB** (США), **Universal Impact Factor** (Австралия).

Статьи, поступившие в редакцию, рецензируются. За достоверность сведений, изложенных в статьях, ответственность несут авторы публикаций.
Мнение редакции может не совпадать с мнением авторов материалов.

Адрес редакции: 831 04, Словакия, г. Братислава, Нове Место, ул. Стара Вайнорска, 1367/4

Сайт журнала: http://ejournal8.com/
E-mail: aphr2010@mail.ru

Учредитель и издатель: Academic Publishing House Researcher s.r.o.

Дата выпуска 15.03.17.
Формат 21 × 29,7/4.

Гарнитура Georgia.

Заказ № 15.

© European Journal of Molecular Biotechnology, 2017

CONTENTS

Articles and Statements

Copyright © 2017 by Academic Publishing House Researcher s.r.o.

Published in the Slovak Republic
European Journal of Molecular Biotechnology
Has been issued since 2013.
ISSN: 2310-6255
E-ISSN: 2409-1332
2017, 5(1): 4-10

DOI: 10.13187/ejmb.2017.1.4
www.ejournal8.com

Articles and Statements

A High-Throughput PCR-Amplification of GC-Rich DNA Sequences

Alexey S. Afoshin [a, *], Philipp V. Kochetkov [a], Zhanna I. Andreeva-Kovalevskaya [a], Zhanna I. Budarina [a], Marina V. Zakharova [a], Alexander V. Lisov [a], Andrey M. Shadrin [a, b], Alexey A. Leontievsky [a, b]

[a] G. K. Skryabin Institute of Biochemistry and Physiology of Microorganisms, Russian Academy of Sciences, Russian Federation
[b] Pushchino State Institute of Life Sciences, Russian Federation

Abstract

The PCR amplification of DNA molecules with a high GC content is a complex procedure and often requires optimisation. In last few years several improvements have been developed to facilitate the optimisation of PCR steps. In this work, five high-fidelity commercial DNA-polymerases for the amplification of GC-rich genes were tested. Using the most effective DNA polymerase, we were able to PCR amplify 161 of 187 (87 %) of target genes with a GC content from 57 to 77 % mostly up to 2500 bp long without an optimisation steps. The final yield of specific PCR products was more than 150 ng from 100 µL PCR reactions mix after the purification of specific DNA products by agarose gel electrophoresis.

Keywords: Actinomyces, PCR, GC-rich, high-throughput, DNA polymerase, dimethyl sulfoxide.

1. Introduction

The microorganisms of the *Actinomycetales* order are able to metabolize hard-to-reach substrates such as chitin (Schrempf, 2001), cellulose (Wilson, 1992), oil (Jirasripongpun, 2002), *etc*. This ability makes actinomycetes a valuable source of the genetic material encoding enzymes applicable in food industry, medicine, agriculture, and different areas of biotechnology. Most of A*ctinomycetales* genomes have a high content of guanine–cytosine pairs (GC), which leads to severe problems with successful PCR amplifications of target genes. There a many protocols based on optimisation of PCR thermal conditions (Orpana et al., 2012), primer design strategy (Li et al., 2011), reaction buffer composition and using special additives (Sahdev et al., 2007; Horakova et al., 2011) have been developed for amplification of GC-rich DNA (Strien et al., 2013; Naz, Fatima, 2013). However, currently there is no sufficient data characterizing the PCR amplification of GC-rich genes for large scale cloning using high-fidelity DNA polymerases. In this work, we test five

* Corresponding authors
E-mail addresses: alex080686@mail.ru (A.S. Afoshin), kochetkov-f@bk.ru (P.V. Kochetkov), hemolysin@rambler.ru (Zh.I. Andreeva-Kovalevskaya), budarina@ibpm.pushchino.ru (Zh.I. Budarina), zemskovam@mail.ru (M.V. Zakharova), ssl208@rambler.ru (A.V. Lisov), andrey2010s@gmail.com (A.M. Shadrin), leont@ibpm.pushchino.ru (A.A. Leontievsky)

high-fidelity DNA-polymerases and describe a system approach on application to the high-throughput PCR-amplification of hundreds of target genes with a high GC content.

2. Materials and Methods

Bacterial strains

Nocardiopsis synnemataformans VKM Ac-2518; *Streptomyces avermitilis* VKM Ac-1301; *Streptomyces mobaraensis* VKM Ac-928; *Saccharopolyspora erythraea* VKM Ac-1189; *Saccharopolyspora rectivirgula* VKM Ac-810; *Saccharothrix espanaensis* VKM Ac-1969; *Meiothermus ruber* VKM B-1258; *Thermomonospora curvata* VKM Ac-1241; *Nocardiopsis alba* VKM Ac-1883 strains with sequenced genomes obtained from All-Russian Collection of Microorganisms (VKM).

Dendrogram construction

The dendrogram was based on 16S ribosomal RNA genes sequences and constructed via BLAST (http://blast.ncbi.nlm.nih.gov) using the fast minimum evolution method for clustering (Desper, Gascuel, 2004).

DNA extraction

For the extraction of total DNA, 1–2 g of the biomass of the bacterial strain was homogenised with 2 ml of phenol and liquid nitrogen in the mortar box. The mixture was transferred into 20 ml of buffer containing 20 mM Tris-HCl, pH 8.0, and 20 mM EDTA and extracted four times with one volume of phenol–chloroform–isoamyl alcohol mixture (25 : 24 : 1). After the extraction, the residual amounts of phenol were removed by chloroform extraction. Purified DNA was precipitated with ethanol and dissolved in 200 μL of mQ water. From one to ten nanograms of DNA was used for a single PCR reaction (50 μL).

Primers Design

Primers were designed in accordance with the following requirements: (i) the Tm value determined by OligoAnalyzer 3.1 software (http://eu.idtdna.com/calc/analyzer) must be in the range from +55°C to +60°C; (ii) the melting temperatures of hairpin loops must be lower than +40°C; (iii) the oligonucleotide length must be at least 15 bp or longer. If one of the oligonucleotide parameters did not comply with the above requirements, the annealing region was shifted 10–20 bp further from the open reading frame of the target gene. This procedure can be automated using a Primer3 oligonucleotide design tool (http://bioinfo.ut.ee/?page_id=163&lang=en) (Untergasser et al., 2012, Koressaar, Remm, 2007). DNA oligonucleotides were synthesized by the Evrogen company service.

PCR conditions

DNA amplification was carried out using a C1000Touch PCR machine (BioRad). For each DNA-polymerase a specific program was used. For Q5 polymerase (cat. no. #M0491S, New England Biolabs): initial denaturation at 98°C (30 s); 35 cycles: 98°C (10 s), 60°C (20 s), 72°C (45 s); final elongation 3 min. For Phusion (cat. no. #M0530S, New England Biolabs): initial denaturation at 98°C (30 s); 30 cycles: 98°C (10 s), 55°C (30 s), 72°C (45 s); final elongation 7 min. For TaqSE (cat. no. E314, SibEnzyme): initial denaturation at 95°C (3 min); 35 cycles: 93°C (30 s), 60°C (30 s), 72°C (1.5 min); final elongation 3 min. For Herculase II (cat. no. 600675, Agilent Technologies): initial denaturation at 98°C (2 min); 35 cycles: 98°C (20 s), 60°C (20 s), 72°C (45 s); final elongation 3 min. For PfuUltra II Fusion HS (cat. no. 600670, Agilent Technologies): initial denaturation at 98°C (2 min); 35 cycles: 98°C (20 s), 60°C (20 s), 72°C (30 s); final elongation 3 min. 0.5 μM oligonucleotide primers used for all DNA-polymerases.

3. Results and discussion

As a source of GC-rich templates, we used a collection of highly diverse microorganisms consisting of eight representatives of the *Actinomycetales* order and one strain of the *Thermales* order with available genome sequences in NCBI database (Fig. 1).

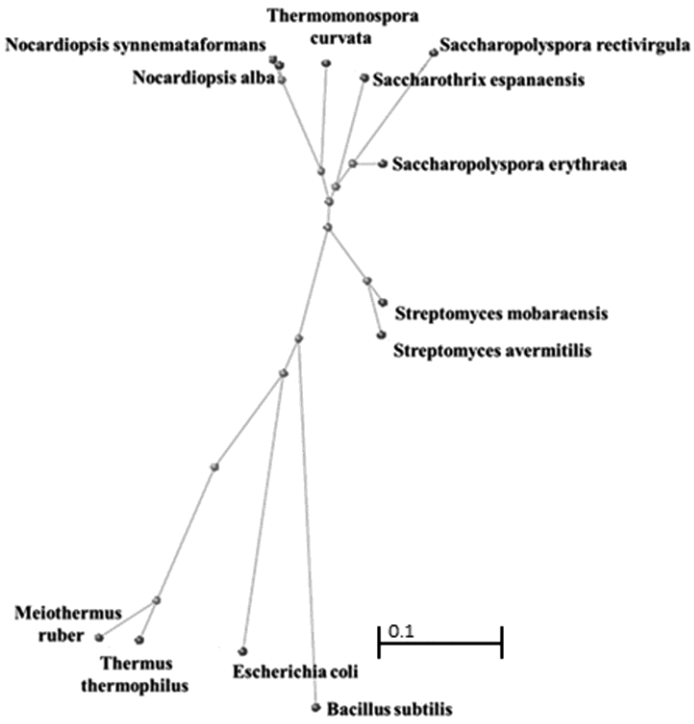

Fig. 1. Radial dendrogram showing the phylogenetic distance between the strains based on nucleotide sequences of 16 rRNA genes.

Table 1. Properties of tested high-fidelity DNA polymerases

Polymerase	Additive	Positive reactions	Error rate*	Price per reaction
Q5	Q5® High GC Enhancer	14 (88%)	100x	$$
Phusion	GC® Reaction Buffer	10 (63%)	50x	$$
TaqSE	No Q5® High GC Enhancer 3% DMSO	2 (13%) 8 (50%) 8 (50%)	n.d.	$
Herculase II Fusion	No Q5® High GC Enhancer 3% DMSO	2 (13%) 15 (94%) 15 (94%)	7x	$$
PfuUltra II Fusion HS	No Q5® High GC Enhancer 3% DMSO	1 (6%) 7 (44%) 7 (44%)	20x	$$$

Information taken from vendors web sites.
*) Error rate shown, relative to Taq-polymerase. n.d. – no data.

The most effective DNA polymerase was determined by testing five commercially available high-fidelity DNA polymerases on 16 target genes of the *Saccharopolyspora erythraea* (VKM Ac-1189) and *Nocardiopsis alba* (VKM Ac-1883) strains (Fig. 2). Q5 DNA polymerase in the presence of the *High GC enhancer* amplifies 14 of 16 target genes (Fig. 2A), whereas Phusion DNA polymerase in GC-reaction buffer amplifies only 10 of 16 genes with a greater amount of nonspecific products (Fig. 2B). TaqSE, Herculase II, and PfuUltra II Fusion HS DNA polymerases supplied without any special buffer or a reagent for amplification of a GC-rich DNA. In the PCRs with the standard buffers the specific products were detected only for one or two of 16 tested genes (Fig. 2C-E). These results are in agreement with the previously reported observation for Taq DNA-polymerase (Naz, Fatima, 2013).

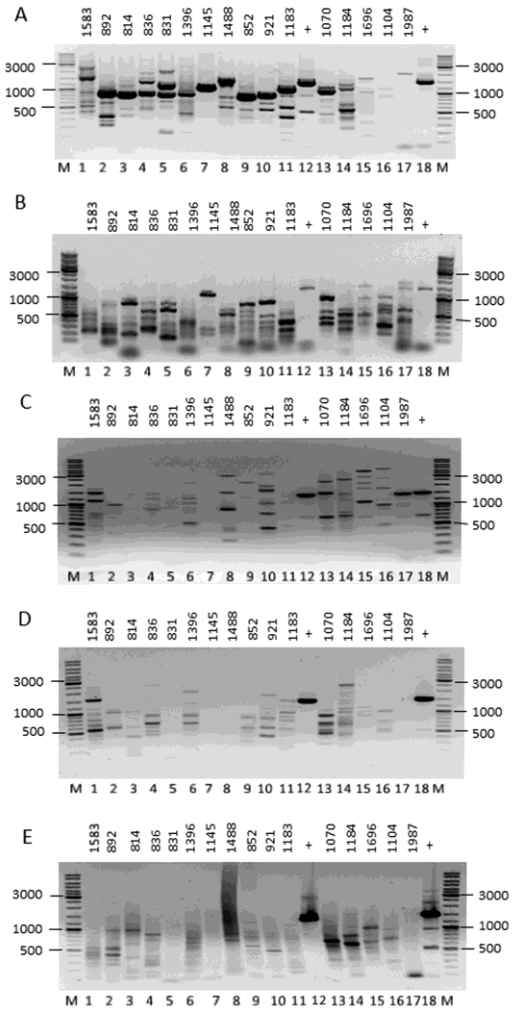

Fig. 2. Results of testing five different high-fidelity DNA polymerases on GC-rich templates. (A) Q5 polymerase; (B) Phusion; (C) TaqSE; (D) Herculase II; (E) PfuUltra II Fusion HS. M – DNA ladder (cat. no. SM0331; Thermo Scientific); tracks from 1 to 11 contain reactions for amplicons of the *Saccharopolyspora erythraea* VKM Ac-1189 strain; tracks from 13 to 17 contain reactions for amplicons from 183 to 187 (sup. Table 1) of the *Nocardiopsis Alba* VKM Ac-1883 strain. Tracks 12 and 18 contain the products of 16S ribosomal RNA gene amplification as positive controls for *Saccharopolyspora erythraea* VKM Ac-1189 and *Nocardiopsis Alba* VKM Ac-1883 strains, respectively. The molecular weight of specific PCR product indicated above the track.

Some additives and company-specific reagents can significantly increase the success of amplification of a GC-rich DNA (Strien et al., 2013; Naz, Fatima, 2013). We repeat the reactions with TaqSE, Herculase II, and PfuUltra II Fusion HS DNA polymerases in presence of *High GC enhancer* and 3 % DMSO. The number of amplified specific products increases up to 10-fold. From eight for TaqSE polymerase to fifteen for Herculase II with 3 % DMSO (Table 1). The pattern of amplified products on agarose gels was slightly different for reactions supplemented with *High GC-enhancer* and 3 % DMSO for same DNA-polymerase (Fig. 3).

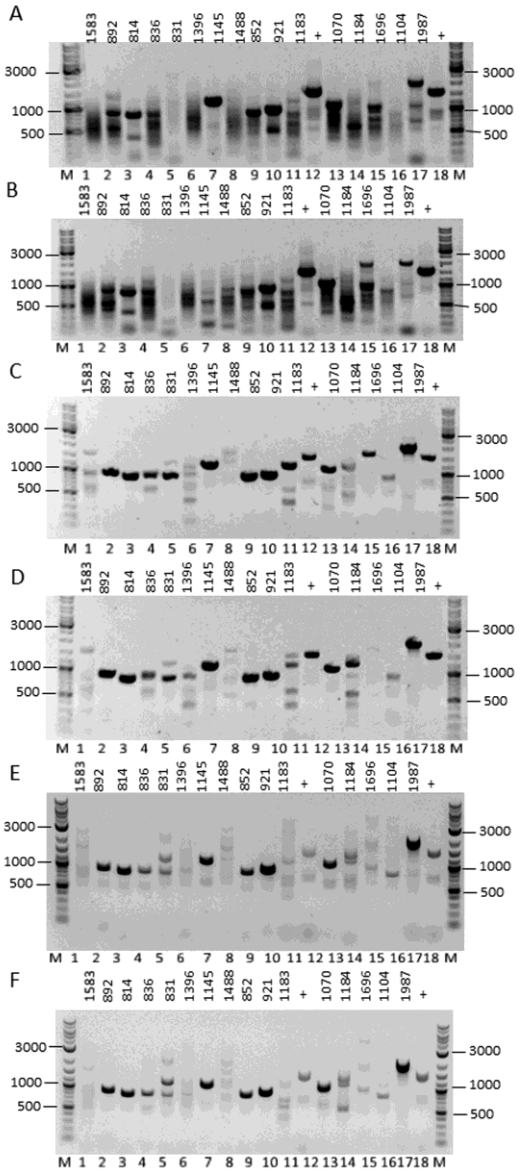

Fig. 3. Results of testing TaqSE (A,B); Herculase II (C,D); PfuUltra II Fusion HS (E,F) in presence of *High GC-enhancer* (A,C,E) and 3 % DMSO (B,D,F). The reactions have same positions as described for Fig. 1.

Because Q5 DNA polymerase amplify large number of the target genes and has higher fidelity in comparison with Herculase II, we test Q5 enzyme for the ability to amplify 187 target genes. The PCR amplifications considered as a successful when at least 150 ng of specific DNA recovered from 100 µL of the PCR reaction mixture purified from the specific DNA band of agarose gel by a QIAgen gel extraction kit (cat. no. 28706). In our conditions, 161 (87 %) target genes successfully amplified.

In eight of nine strains, the number of amplified genes was higher than 79 % (Fig. 4A). For two of nine strains, 100 % of target products successfully amplified. In the case of the *Thermomonospora curvata* VKM Ac-1241 strain, the number of amplified genes was 60 %, because only six of ten reactions gave the sufficient yield of the target DNA. However, in three of four negative reactions, the specific PCR products detected on the agarose gel. This observation indicates that the amount of successfully amplified genes can be increased via the optimisation of PCR conditions.

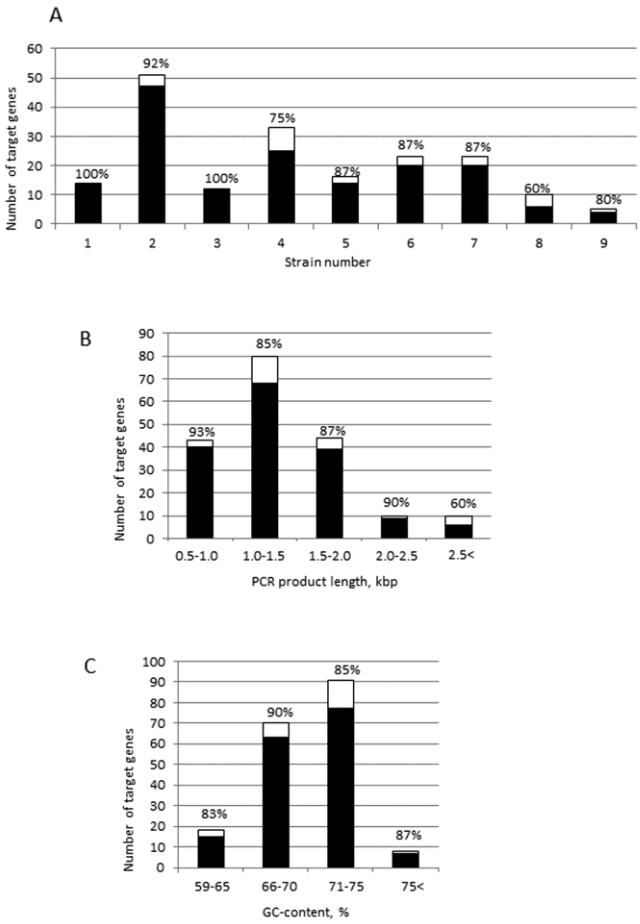

Fig. 4. Correlation between the number of successfully amplified genes and the parameters of DNA amplification. The number of successfully amplified genes shown as black fraction of the columns. The ratio between successfully amplified genes and total number of genes in the set shown above the columns. (A) Dependence on the specificity of the strains: 1 – *Nocardiopsis synnemataformans* VKM Ac-2518 (GC content 72.3 %); 2 – *Streptomyces avermitilis* VKM Ac-1301 (GC content 70.7 %); 3 – *Streptomyces mobaraensis* VKM Ac-928 (GC content 73.3 %); 4 – *Saccharopolyspora erythraea* VKM Ac-1189 (GC content 71.1 %); 5 – *Saccharopolyspora rectivirgula* VKM Ac-810 (GC content 68.9 %); 6 – *Saccharothrix espanaensis* VKM Ac-1969 (GC content 72.2 %); 7 – *Meiothermus ruber* VKM B-1258 (GC content 63.4 %); 8 – *Thermomonospora curvata* VKM Ac-1241 (GC content 71.6 %); 9 – *Nocardiopsis alba* VKM Ac-1883 (GC content 69.6 %). The average GC content in the amplified target genes for each strain is given in brackets. (B) Dependence on the length of target genes. (C) – Dependence on the GC content in the target genes.

The lengths of amplified target genes were in the range from 592 to 3834 bp. The target genes up to 2500 bp long successfully amplified. For products longer than 2500 bp, the portion of amplified genes decreased from 90±3 % to 60 % (Fig. 4B). Presumably, the amplification of long target genes can be improved by increasing the elongation time. However, for high-throughput amplification procedures where the majority of target genes (95 % in our set) are shorter than 2500 bp, we recommend to use a 45-s PCR elongation step to prevent the synthesis of nonspecific products.

The GC content in the whole set of amplified target sequences varied from 57 to 77 %, and the majority (86 %) of target sequences contained from 66 to 75 % GC residues (Fig. 4C). In our set of PCR procedures, we did not identify any significant correlation between the amplification efficiency and the GC content of target genes.

4. Conclusion

Summing up, our results show that Herculase II and Q5 DNA polymerases are most effective high-fidelity DNA polymerases for high-throughput amplification of large number of GC-rich target genes. Presence of additives such us *High GC-enhancer* or DMSO is necessary for successful amplifications of GC-rich DNA. Together with the primer design procedure, our approach affords 87 % of successful amplifications of target genes in amounts sufficient for downstream applications such as cloning, restriction analysis, sequencing, *etc*. The absence of optimisation allows one to apply this protocol for the high-throughput cloning of *Actinomycetales* genetic material and other GC-rich genes.

5. Acknowledgments

This work was supported by the Ministry of Education and Science of the Russian Federation (project no. RFMEFI60714X0013) [Agreement No. 14.607.21.0013]. A.S.A. was supported by the Foundation for Assistance to Small Innovative Enterprises in Science and Technology (project no. 5843 GU 2015 of 10.06.2015).

References

Desper, Gascuel, 2004 – *Desper, R., Gascuel, O.* (2004). Theoretical foundation of the balanced minimum evolution method of phylogenetic inference and its relationship to weighted least-squares tree fitting. *Mol. Biol. Evol.* Vol. 21, № 3. pp. 587-598.

Horakova et al., 2011 – *Horakova, H., Polakovicova, I., Shaik, G.M., Eitler, J., Bugajev, V., Draberova, L., Draber, P.* (2011). 1,2-propanediol-trehalose mixture as a potent quantitative real-time PCR enhancer. *BMC Biotechnology*. Vol. 11, № 4. pp. 1-6.

Jirasripongpun, 2002 – *Jirasripongpun, K.* (2002). The characterization of oil-degrading microorganisms from lubricating oil contaminated (scale) soil. *Lett. Appl. Microbiol.* Vol. 35, № 4. pp. 296-300.

Koressaar, Remm, 2007 – *Koressaar, T., Remm, M.* (2007). Enhancements and modifications of primer design program Primer3. *Bioinformatics*. Vol. 23, № 10. pp. 1289-1291.

Li et al., 2011 – *Li, L.Y., Li, Q., Yu, H., Zhong, M., Yang, L., Wu, Q.H., Qiu, Y.R., Luo, S.Q.* (2011). A primer design strategy for PCR amplification of GC-rich DNA sequences. *Clinical Biochemistry*. Vol. 44, № 8-9. pp. 692–698.

Naz, Fatima, 2013 – *Naz, S., Fatima, A.* (2013). Amplification of GC-rich DNA for high-throughput family based genetic studies. *Mol. Biotechnol.* Vol. 53, № 3. pp. 345–350.

Orpana et al., 2012 – *Orpana, A.K., Ho, T.H., Stenman, J.* (2012). Multiple Heat Pulses during PCR Extension Enabling Amplification of GC-Rich Sequences and Reducing Amplification Bias Anal. Chem. Vol. 84, № 4. pp. 2081–2087.

Sahdev et al., 2007 – *Sahdev, S., Saini, S., Tiwari, P., Saxena, S., Saini, K.S.* (2007). Amplification of GC-rich genes by following a combination strategy of primer design, enhancers and modified PCR cycle conditions. *Molecular and Cellular Probes*. Vol. 21, № 4. pp. 303–307.

Schrempf, 2001 – *Schrempf, H.* (2001). Recognition and degradation of chitin by streptomycetes. *Antonie Van Leeuwenhoek*. Vol. 79, № 3. pp. 285-289.

Strien et al., 2013 – *Strien, J., Sanft, J., Mall, G.* (2013). Enhancement of PCR amplification of moderate GC-containing and highly GC-rich DNA sequences. *Mol. Biotechnol.* Vol. 54, № 3. pp. 1048-1054.

Untergasser et al., 2012 – *Untergasser, A., Cutcutache, I., Koressaar, T., Faircloth, J.Ye, B.C., Remm, M., Rozen, S.G.* (2012). Primer3-new capabilities and interfaces. *Nucleic Acids Res.* Vol. 40, № 15. pp. 1-12.

Wilson, 1992 – *Wilson, D.B.* (1992). Biochemistry and genetics of actinomycete cellulases. *Crit. Rev. Biotechnol.* Vol. 12, № 1-2. pp. 45-63.

Copyright © 2017 by Academic Publishing House Researcher s.r.o.

Published in the Slovak Republic
European Journal of Molecular Biotechnology
Has been issued since 2013.
ISSN: 2310-6255
E-ISSN: 2409-1332
2017, 5(1): 11-22

DOI: 10.13187/ejmb.2017.1.11
www.ejournal8.com

Distribution of Molecules of ZEOLITH detox and ZEOLITH Crème in Water as Factor for Health

Ignat Ignatov [a, *]

[a] Scientific Research Center of Medical Biophysics, Sofia, Bulgaria

Abstract

We studied the mathematical model of interaction with water of natural mineral and microporous crystalline mineral ZEOLITH detox and ZEOLITH Creme of LavaVitae Company (Austria). In this report are submitted data about the interaction of ZEOLITH detox and ZEOLITH Creme with water, obtained by non-equilibrium (NES) and differential-equilibrium energy spectrum (DNES) of water. The average energy ($\Delta E_{H...O}$) of hydrogen H...O-bonds among individual molecules H_2O after treatment of ZEOLITH detox with water measured by NES- and DNES-methods is ΔE=-0.0034±0.0011 eV for ZEOLITH detox. The average energy ($\Delta E_{H...O}$) of hydrogen H...O-bonds among individual molecules H_2O after treatment of ZEOLITH detox with water measured by NES- and DNES-methods is ΔE=-0.0034±0.0011 eV for ZEOLITH detox. The average energy ($\Delta E_{H...O}$) of hydrogen H...O-bonds among individual molecules H_2O after treatment of ZEOLITH detox with water measured by NES- and DNES-methods is ΔE=-0.007±0.0011 eV for ZEOLITH Creme. These results suggest the restructuring of $\Delta E_{H...O}$ values among H_2O molecules with a statistically reliable increase of local extremums in DNES-spectra. The research is performed for ZEOLITH detox with study of pH and oxidative reduction potential (ORP).

Keywords: ZEOLITH detox, ZEOLITH Creme, nanostructures, mathematical model, NES, DNES.

1. Introduction

The ZEOLITH detox is mineral refers to new generation of natural mineral sorbents (NMS). Zeolites are the alumosilicate members of the family of microporous solids known as "molecular sieves", named by their ability to selectively sort molecules based primarily on a size exclusion process. Natural zeolites form when volcanic rocks and ash layers react with alkaline groundwater. Zeolites also crystallize in post-depositional environments over periods ranging from thousands to millions of years in shallow marine basins. Naturally occurring zeolites are rarely pure and are contaminated to varying degrees by other minerals, metals, quarts, or other zeolites. For this reason, naturally occurring zeolites are excluded from many important commercial applications where uniformity and purity are essentials.

As natural mineral zeolite has unusually broad scope of application in industry. Adsorption, catalytic, and reduction-oxidation Zeolites is widely used in industry as a desiccant of gases and liquids, for treatment of drinking and sewage water from heavy metals, ammonia, phosphorus, as

* Corresponding author
E-mail addresses: mbioph@dir.bg (I. Ignatov)

catalyst in petrochemical industry for benzene extraction, for production of detergents and for extracting of radionuclides in nuclear reprocessing. It is also used in medicine as nutritional supplements having antioxidant properties. Some authors make qualifications of zeolites as nano materials.

A wide range of properties of zeolite defines the search for new areas of industrial application of these minerals in science and nano technology that contributes to a deeper study the mechanism of interaction of these minerals with water. The company LavaVitae produces ZEOLITH Creme with exceptional results on the skin and skin diseases. This paper deals with evaluating of mathematical models of interaction of ZEOLITH detox and ZEOLITH Creme with water.

2. Materials and Methods

2.1. Materials

The study is performed with samples of ZEOLITH detox ZEOLITH Creme from LavaVitae Company.

There are valid the following methods for research of zeolite.

2.2. Analytical Methods

The analytical methods were accredited by the Institute of Geology of Ore Deposits. Petrography, Mineralogy, and Geochemistry (Russian Academy of Sciences). Samples were treated by various methods as ICP-OES, GC, and SEM.

2.3. Gas-Chromatography

Gas-chromatography (GC) is performed at Main Testing Centre of Drinking Water (Moscow, the Russian Federation) on Kristall 4000 LUX M using Chromaton AW-DMCS and Inerton-DMCS columns (stationary phases 5% SE-30 and 5% OV-17), equipped with flame ionization detector (FID) and using helium (He) as a carrier gas.

2.4. Inductively Coupled Plasma Optical Emission Spectrometry (ICP-OES)

The mineral composition is studied by inductively coupled plasma optical emission spectrometry (ICP-OES) on Agilent ICP 710-OES (Agilent Technologies, USA) spectrometer, equipped with plasma atomizer (under argon stream), MegaPixel CCD detector, and 40 MHz free-running, air-cooled RF generator, and Computer-optimized exhale system: the spectral range at 167–785 nm; plasma gas: 0–22.5 l/min in 1.5 l/min; power output: 700–1500 W in 50 W increments.

2.5. Transmission Electron Microscopy (TEM)

The structural studies were carried out with using JSM 35 CF (JEOL Ltd., Korea) device, equiped with X-ray microanalyzer "Tracor Northern TN", SE detector, thermomolecular pump, and tungsten electron gun (Harpin type W filament, DC heating); working pressure: 10^{-4} Pa (10^{-6} Torr); magnification: 300.000, resolution: 3.0 nm, accelerating voltage: 1–30 kV; sample size: 60–130 mm.

2.6. IR-Spectrospopy

IR-spectra of water samples, obtained after being contacted 3 days with shungite and zeolite, are registered on Fourier-IR spectrometer Brucker Vertex ("Brucker", Germany) (a spectral range: average IR – 370–7800 cm^{-1}; visible – 2500–8000 cm^{-1}; the permission – 0.5 cm^{-1}; accuracy of wave number – 0.1 cm^{-1} on 2000 cm^{-1});

For the research of ZEOLITH detox and ZEOLITH Creme the methods are:

2.7. Non-equilibrium Spectrum (NES) and Differential Non-equilibrium Spectrum (DNES)

The energy spectrum of water is characterized by a non-equilibrium process of water droplets evaporation, therefore, the term non-equilibrium spectrum (NES) of water is used. The difference

$\Delta f(E) = f$ *(samples of water)* $- f$ *(control sample of water)* – is called the "differential non-equilibrium energy spectrum of water" (DNES).

2.8. Measurement of pH and ORP (oxidative-redox potential)

The research is performed from Georgi Gluhchev with device from Hanna Instruments.

3. Results and Discussion

In comparison with zeolite comprises a microporous crystalline aluminosilicate mineral commonly used as commercial adsorbents, three-dimensional framework of which is formed by linking via the vertices the tetrahedral $[AlO_4]^{2-}$ and $[SiO_4]^{2-}$ (Panayotova, Velikov, 2002). Each tetrahedron $[AlO_4]^{2-}$ creates a negative charge of the carcasses compensated by cations (H^+, Na^+, K^+, Ca^{2+}, NH_4^+, etc.), in most cases, capable of cation exchange in solutions. Tetrahedrons formed the secondary structural units, such as six-membered rings, five-membered rings, truncated octahedra, etc. Zeolites framework comprise interacting channels and cavities forming a porous structure with a pore size of 0.3–1.0 nm. Average crystal size of the zeolites may range from 0.5 to 30 μm.

By the measurement of IR spectra in the range of vibrations in the crystal mineral framework one can obtain the information: a) on the structure of the framework, particularly type lattice ratio SiO_2/Al_2O_3, nature and location of cations and changes in the structure in the process of the thermal treatment; b) on the nature of the surface of the structural groups, which often serve as adsorption and catalytically active sites.

Other method for obtaining information about the average energy of hydrogen bonds in an aqueous sample is measuring of the spectrum of the water state. It was established experimentally that at evaporation of water droplet the contact angle θ decreases discretely to zero, whereas the diameter of the droplet changes insignificantly (Antonov, 1995). By measuring this angle within a regular time intervals a functional dependence f(θ) can be determined, which is designated by the spectrum of the water state (Ignatov, 2005; Ignatov, 2012; Ignatov & Mosin, 2013). For practical purposes by registering the spectrum of water state it is possible to obtain information about the averaged energy of hydrogen bonds in an aqueous sample. For this purpose the model of W. Luck was used, which consider water as an associated liquid, consisted of O–H...O–H groups (Luck et al., 1980). The major part of these groups is designated by the energy of hydrogen bonds (-E), while the others are free (E = 0). The energy distribution function f(E) is measured in electron-volts (eV^{-1}) and may be varied under the influence of various external factors on water as temperature and pressure.

For calculation of the function f(E) experimental dependence between the water surface tension measured by the wetting angle (θ) and the energy of hydrogen bonds (E) is established:

$$f(E) = b\, f(\theta) / 1 - (1 + b\, E)^2)^{1/2}, \text{ where } b = 14.33\ eV^{-1};\ \theta = \arccos(-1 - b\, E)$$

The energy of hydrogen bonds (E) measured in electron-volts (eV) is designated by the spectrum of energy distribution. This spectrum is characterized by non-equilibrium process of water droplets evaporation, thus the term “non-equilibrium energy spectrum of water” (NES) is applied.

The difference Δf(E) = f (samples of water) – f (control sample of water) – is designated the “differential non-equilibrium energy spectrum of water” (DNES).

DNES is calculated in milli-electron volts (0.001 eV or meV) is a measure of changes in the structure of water as a result of external factors. The cumulative effect of all other factors is the same for the control sample of water and the water sample, which is under the influence of this impact. The research with NES method of water drops received after 3 days stay with zeolite in deionized water may also give valuable information on the possible number of hydrogen bonds as percent of water molecules with different values of distribution of energies. These distributions are basically connected with restructuring of H_2O molecules with the same energies.

3.1. Results with spectral analysis of 1% solution of ZEOLITH detox

The average energy ($E_{H...O}$) of hydrogen H...O-bonds among individual H_2O molecules in 1% solution of ZEOLITH detox is measured at E=-0.1219 eV. The result for the control sample (deionized water) is E=-0.1185 eV. The results obtained with the NES method are recalculated with the DNES method as a difference of the NES (1% solution of ZEOLITH detox) minus the NES (control sample with deionized water) equaled the DNES spectrum of 1% solution of ZEOLITH

detox. Thus, the result for 1% solution of ZEOLITH detox recalculated with the DNES method is ΔE=-0.0034±0.0011 eV. The result shows the increasing of the values of the energy of hydrogen bonds in 1% solution of ZEOLITH detox regarding the deionized water. The result is effect of stimulation on human body. This shows restructuring of water molecules in configurations of clusters, which influence usefully on human health on molecular and cellular level. The effects are describing with mathematical model of 1% solution of ZEOLITH detox.

3.2. Mathematical model of ZEOLITH detox

The research with the NES method of water drops is received with 1% solution ZEOLITH detox, and deionized water as control sample. The mathematical models of 1% solution ZEOLITH detox gives the valuable information for the possible number of hydrogen bonds as percent of H_2O molecules with different values of distribution of energies (Table 1 and Fig. 1). These distributions are basically connected with the restructuring of H_2O molecules having the same energies.

Table 1. The distribution (%, $(-E_{value})/(-E_{total\ value})$ of H_2O molecules in 1 % water solution of ZEOLITH detox (product of LavaVitae, Austria) and control deionized water

-E(eV) x-axis	1% water solution ZEOLITH detox (LavaVitae) y-axis (%((-E_{value}) */ (-$E_{total\ value}$)**	Control Sample Deionized water y-axis (%((-E_{value})*/ (-$E_{total\ value}$)**	-E(eV) x-axis	1% water solution ZEOLITH detox (LavaVitae) y-axis (%((-E_{value}) */ (-$E_{total\ value}$)**	Control Sample Deionized water y-axis (%((-E_{value})*/ (-$E_{total\ value}$)**
0.0937	0	6.7	0.1187	0	15.5
0.0962	0	6.7	0.1212	**18.9**[2]	0
0.0987	0	6.7	0.1237	0	6.7
0.1012	6.0	15.5	0.1262	0	6.7
0.1037	12.5	6.7	0.1287	0	0
0.1062	0	6.7	0.1312	0	3.3
0.1087	3.1	0	0.1337	12.5	0
0.1112	**3.1**[1]	0	0.1362	12.5	3.3
0.1137	0	15.5	0.1387	**18.9**[3]	0
0.1162	12.5	0	–	–	–

Notes:
E=-0.1212 eV is the local extremum for anti-inflammatory effect
E= -0.1387 eV is the local extremum for inhibition of development of tumor cells of molecular level
Notes:
* The result (-E_{value}) is the result of hydrogen bonds energy for one parameter of (-E)
** The result (-E_{value}) is the total result of hydrogen bonds energy

Figure 1 shows the distribution (%, $(-E_{value})/(-E_{total\ value})$ of H_2O molecules in and 1 % of water solution of ZEOLITH detox (product of LavaVitae, Austria) (red line) and control sample deionized water (blue line).

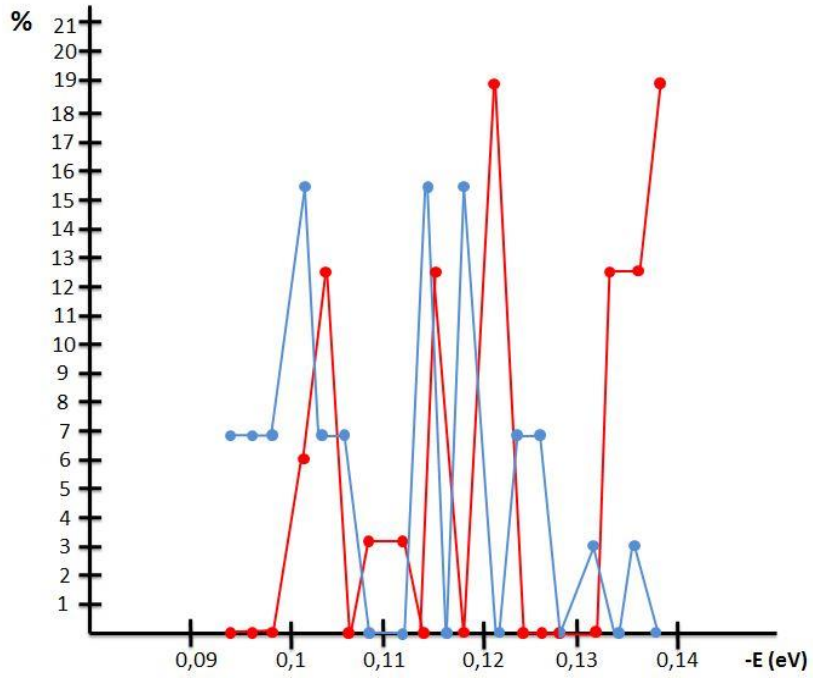

Fig. 1. Mathematical model (Ignatov, Mosin, 2013) of 1 % water solution of ZEOLITH detox (product of LavaVitae, Austria)

Notes:
E=-0.1212 eV is the local extremum for anti-inflammatory effect
E= -0.1387 eV is the local extremum for inhibitation of development of tumor cells of molecular level

The experimental data obtained testified the following conclusions from the mathematical model of in 1 % water solution of ZEOLITH detox (product of LavaVitae, Austria) and control deionized water. The distribution (%, $(-E_{value})/(-E_{total\ value})$ of water molecules in mathematical model of in 1 % water solution of ZEOLITH detox (product of LavaVitae, Austria) and control deionized water. The distribution (%, $(-E_{value})/(-E_{total\ value})$ of water molecules in ZEOLITH detox (product of LavaVitae, Austria) according control sample is different. However, for the value E = -0.1387 eV or λ = 8.95 μm there is the biggest local extremum (18.9 (%, $(-E_{value})/(-E_{total\ value})$) corresponding to the re-structuring of hydrogen bonds among H_2O molecules for inhibition of development of tumor cells of molecular level. This difference may indicate on the different number of hydrogen bonds in water samples, as well as their physical parameters (pH, ORP), resulting in different distribution of H_2O molecules and different values of H_2O molecules with ratios of $(-E_{value})/(-E_{total\ value})$. Particularly it was observed the statistical re-structuring of H_2O molecules in water samples according to the energies. The experimental data may prove that stipulates the restructuring of H_2O molecules on molecular level and may be used for the prophylaxis of development of tumor cells. For the value E=-0.1212 eV or λ=10.23 μm there is the bigger local extremum (18.9 (%, $(-E_{value})/(-E_{total\ value})$) corresponding to the re-structuring of hydrogen bonds among H_2O molecules for anti-inflammatory effect.. The experimental data for ZEOLITH detox may prove that stipulates the restructuring of H_2O molecules on molecular level and the biophysical effects are:

E=-0.1212 eV is the local extremum for anti inflammatory effect

E= -0.1387 eV is the local extremum for inhibition of development of tumor cells of molecular level

3.3. Results with spectral analysis of 1% solution of ZEOLITH Creme

The average energy ($E_{H...O}$) of hydrogen H...O-bonds among individual H_2O molecules in 1 % solution of ZEOLITH Creme is measured at E=-0.1200 eV. The result for the control sample (deionized water) is E=-0.1130eV. The results obtained with the NES method are recalculated with

the DNES method as a difference of the NES (1 % solution of ZEOLITH Creme) minus the NES (control sample with deionized water) equaled the DNES spectrum of 1 % solution of ZEOLITH Creme. Thus, the result for 1 % solution of ZEOLITH Creme recalculated with the DNES method is ΔE=-0.007±0.0011 eV. The result shows the increasing of the values of the energy of hydrogen bonds in 1 % solution of ZEOLITH detox regarding the deionized water. The result is effect of stimulation on human body. The result is 6.4 times more than statistical reliable result. This shows restructuring of water molecules in configurations of clusters, which influence usefully on human health on molecular and cellular level. The effects are describing with mathematical model of 1 % solution of ZEOLITH Creme.

3.2. Mathematical model of ZEOLITH detox

The research with the NES method of water drops is received with 1% solutions ZEOLITH Creme and deionized water as control samples. The mathematical models of 1% solution ZEOLITH Creme give the valuable information for the possible number of hydrogen bonds as percent of H_2O molecules with different values of distribution of energies (Table 1). These distributions are basically connected with the restructuring of H_2O molecules having the same energies.

3.3. Mathematical model of ZEOLITH Creme (product of the company LavaVitae)

The research with the NES method of water drops is received with 1 % solution ZEOLITH Creme, and deionized water as control sample. The mathematical model of 1 % solution ZEOLITH Creme gives the valuable information for the possible number of hydrogen bonds as percent of H_2O molecules with different values of distribution of energies (Table 2 and Fig. 2). These distributions are basically connected with the restructuring of H_2O molecules having the same energies.

Table 2. The distribution (%, $(-E_{value})/(-E_{totalvalue})$ of H_2O molecules in 1% water solution of ZEOLITH Creme (product of LavaVitae, Austria) and control deionized water.

-E(eV) x-axis	1% water solution ZEOLITH Creme (LavaVitae) y-axis (%((-E_{value}) */ (-$E_{total\ value}$)**	Control Sample Deionized water y-axis (%((-E_{value})*/ (-$E_{total\ value}$)**	-E(eV) x-axis	1% water solution ZEOLITH Creme (LavaVitae) y-axis (%((-E_{value}) */ (-$E_{total\ value}$)**	Control Sample Deionized water y-axis (%((-E_{value})*/ (-$E_{total\ value}$)**
0.0937	0	0	0.1187	0	5.7
0.0962	0	11.4	0.1212	**15.2**[2]	5.7
0.0987	7.8	5.7	0.1237	3.8	0
0.1012	7.8	5.7	0.1262	3.8	5.7
0.1037	3.8	11.4	0.1287	7.7	5.7
0.1062	7.8	11.4	0.1312	7.7	0
0.1087	3.8	0	0.1337	7.7	0
0.1112	**3.8**[1]	5.7	0.1362	3.8	5.7
0.1137	0	8.8	0.1387	**7.7**[3]	5.7
0.1162	7.8	5.7	–	–	–

Notes:
E=-0.1212 eV is the local extremum for anti-inflammatory effect
Notes:
* The result ($-E_{value}$) is the result of hydrogen bonds energy for one parameter of (-E)
** The result ($-E_{value}$) is the total result of hydrogen bonds energy

Figure 2 shows the distribution (%, $(-E_{value})/(-E_{total\ value})$ of H_2O molecules in and 1 % of water solution of ZEOLITH Creme (product of LavaVitae, Austria) (red line) and control sample deionized water (blue line).

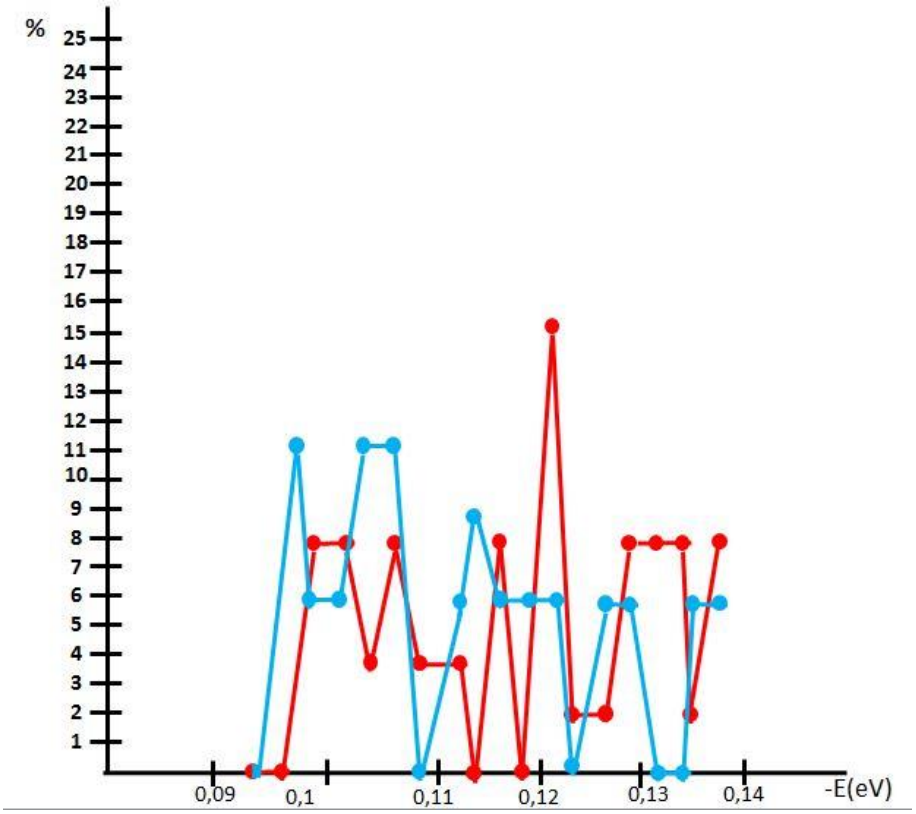

Fig. 2. Mathematicalmodel (Ignatov, Mosin, 2013) of 1% watersolution of ZEOLITH Creme (product of LavaVitae, Austria).
Notes:
E=-0.1212 eV is the local extremum for anti-inflammatory effect

The experimental data obtained testified the following conclusions from the mathematical model of in 1 % water solution of ZEOLITH Creme (product of LavaVitae, Austria) and control deionized water. The distribution (%, $(-E_{value})/(-E_{total\ value})$ of water molecules in mathematical model of in 1 % water solution of ZEOLITH Creme (product of LavaVitae, Austria) and control deionized water. The distribution (%, $(-E_{value})/(-E_{total\ value})$ of water molecules in ZEOLITH Creme (product of LavaVitae, Austria) according control sample is different. However, for the value E = -0.1212 eV or λ = 10.23 μm there is the biggest local extremum (15.2(%, $(-E_{value})/(-E_{total\ value})$) corresponding to the re-structuring of hydrogen bonds among H_2O molecules for inhibition of development of tumor cells of molecular level. This difference may indicate on the different number of hydrogen bonds in water samples, resulting in different distribution of H_2O molecules and different values of H_2O molecules with ratios of $(-E_{value})/(-E_{total\ value})$. Particularly it was observed the statistical re-structuring of H_2O molecules in water samples according to the energies.The experimental data may prove that stipulates the restructuring of H_2O molecules on molecular level and may be used for cleaning of skin with anti inflammatory effect. The experimental data for ZEOLITH Crème may prove that stipulates the restructuring of H_2O molecules on molecular level and the biophysical effect is:

E=-0.1212 eV is the local extremum for anti-inflammatory effect

4. Results with pH and ORP

There are valid the following results of pH as indicator for acid alkaline medium of the products of Lava Vitae. There are the results also of ORP or Oxidation-reduction potential.

The results are for 1 % of solutions of products, which are made from deionized water. This research is performed with Georgi Gluhchev from Bulgarian Academy of Science. The results of pH of deionized water is 6.05 and of ORP is 119.7. Table 3 shows the results of pH and ORP.

Table 3. Results of products of company LavaVitae for pH and ORP

Product	pH	ORP (mV)	Coordinates Fig. 2
VITA Intense	4.07±0.02	- 104.5	Point 1 (4,07; -104.5)
BOOST	3.60±0.02	+113.6	Point 2 (3,90;113.6)
ZEOLITH detox	8.01±0.02	+109.5	Point 3 (8,01;103.3)
Deionized water	6.05±0.02	+119.7	

Figure 3 shows the dependence between the acidity and basicity (pH) of electrochemically activated solutions and the oxidation-reduction potential (ORP). The pH value within the interval from 3 to 10 units and the ORP within the interval from -400 mV to +900 mV characterize the area of the biosphere of microorganisms. Outside these ranges of pH and ORP the microorganisms will hardly survive.

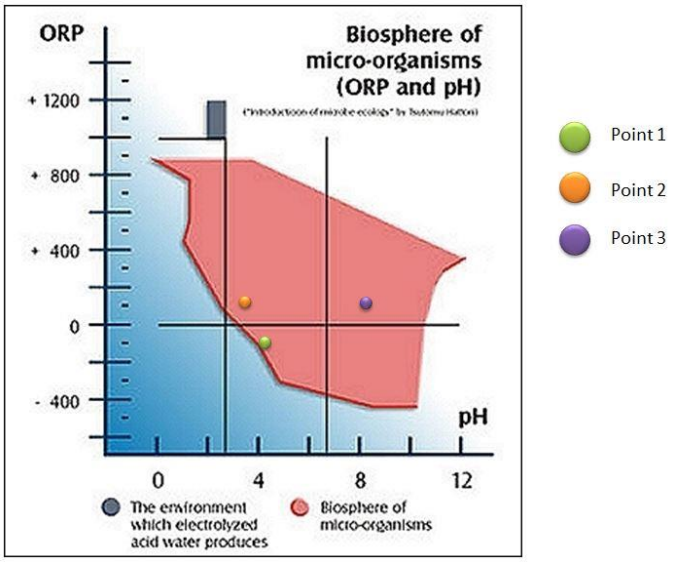

Fig. 3. The dependence between acidity and basicity (pH) of solutions and the ORP on the biosphere of micro-organisms (point 1; VITA intense), (point 2; BOOST), point 3; ZEOLITH detox).

Owing to the unique porous structure the mineral Zeolites are ideal absorbents and fillers (Gorshteyn et al., 1979), and as sorbents have a number of positive characteristics:

- High adsorption capacity, characterized by low resistance to water pressure;
- Mechanical strength and low abrasion resistance;
- Corrosion-resistance;
- Absorption capacity relatives to many substances, both organic (oil, benzene, phenol, pesticides, etc.) and inorganic (chlorine, ammonia, heavy metals);
- Catalytic activity;
- Relatively low cost;
- Environmental friendliness and ecological safety.

5. Discussion and Conclusions

5.1. ZEOLITH detox (product of LavaVitae company)

The interaction of ZEOLITH detox with water is quiet complex and results the restructuring of energy values among H_2O molecules with a statistically reliable increase of local extremums in DNES-spectra after treatment of ZEOLITH detox with water. These values are measured at -0.1219 eV for ZEOLITH detox. The result for control sample (deionized water) is -0.1185 eV. The results with NES method were recalculated by the DNES method. The result of ZEOLITH detox with DNES method is 0.0034±0.0011 eV.

From the NES and DNES spectrum and mathematical model of 1% solution of ZEOLITH detox and deionized water as control sample are valid the following conclusions for biophysical effects for ZEOLITH detox (LavaVitae Company)

- Anti-inflammatory effect;
- inhibition of development of tumor cells of molecular level;

Naturally occurring zeolites are rarely pure and are contaminated to varying degrees by other minerals, metals, quarts, or other zeolites. For this reason, naturally occurring zeolites are excluded from many important commercial applications where uniformity and purity are essential. In comparison with zeolite comprises a microporous crystalline aluminosilicate mineral commonly used as adsorbent. Zeolite$^-$ creates a negative charge of the carcasses compensated by cations (H^+, Na^+, K^+, Ca^{2+}, NH_4^+, etc.), in most cases, capable of cations exchange in solutions. Efficiency of using zeolite is stipulated by the high range of valuable properties (absorption, catalytic, antioxidant, regenerative, antibacterial). There is permanent antioxidant activity of zeolite on enzymes (Dogliotti et al., 2012; Ignatov, Mosin, 2015).

5.2. *ZEOLITH Creme (product of LavaVitae company)*

From the NES and DNES spectrum and mathematical model of 1 % solution of ZEOLITH Crème and deionized water as control sample is valid the following conclusion for biophysical effects for ZEOLITH Creme (LavaVitae company)

- anti-inflammatory effect

Naturally occurring zeolites are rarely pure and are contaminated to varying degrees by other minerals, metals, quarts, or other zeolites. For this reason, naturally occurring zeolites are excluded from many important commercial applications where uniformity and purity are essential. In comparison with zeolite comprises a microporous crystalline aluminosilicate mineral commonly used as adsorbent. Zeolite$^-$ creates negative charge of the carcasses compensated by cations (H^+, Na^+, K^+, Ca^{2+}, NH_4^+,etc.), in most cases, capable of cations exchange in solutions. Efficiency of using zeolite is stipulated by the high range of valuable properties (absorption, catalytic, antioxidant, regenerative, antibacterial). There is permanent antioxidant activity of zeolite on enzymes (Dogliotti et al., 2012; Ignatov, Mosin, 2015).

6. Acknowledgements

The author wish to thank to Georgi Gluhchev for the research of pH and ORP. The author express thankful to Teodora Todorova for the preparation of the figures.

References

Antonov, 1995 – *Antonov, A.* (1995). Research of the Nonequilibrium Processes in the Area in Allocated Systems. *Diss. Thesis Doctor of Physical Sciences. Sofia*: *Blagoevgrad*: pp. 1–255.

Gluhchev et al., 2015a – *Gnluhchev, G., Ignatov, I., Karadzhov, S., Miloshev, G., Ivanov, I., Mosin, O.V.* (2015). Biocidal Effects of Electrochemically Activated Water. *Journal of Health, Medicine and Nursing*, V. 11: pp. 67-83.

Gluhchev et al., 2015b – *Gluhchev, G., Ignatov, I., Karadzhov, S., Miloshev, G., Ivanov, N., Mosin, O.V.* (2015). Electrochemically Activited Water: Biophysical and Biological Effects of Anolyte and Catholyte Types of Water. *European Journal of Molecular Biotechnology*, V.1, pp. 12-26.

Gluhchev et al., 2015c – *Gluhchev, G., Ignatov, I., Karadzhov, S., Miloshev, G., Ivanov, N., Mosin, O.V.* (2015). Studying the Antimicrobial and Antiviral Effects of Electrochemically Activated Nacl Solutions of Anolyte and Catholyte on a Strain of E. Coli DH5 and Classical Swine Fever (CSF) Virus. *European Journal of Medicine*, 9 (3): pp. 124-138.

Gluhchev et al., 2015d – *Gluhchev, G., Ignatov, I., Karadzhov, S., Miloshev, G., Ivanov, I.,*

Mosin, O.V. (2015). Electrochemically Activated Water. Biophysical and Biological Effects of Anolyte and Catholyte as Types of Water. *Journal of Medicine, Physiology and Biophysics*, Vol. 10: pp. 1-17.

Gluhchev et al., 2015e – *Gluhchev, G., Ignatov, I., Karadzhov, S., Miloshev, G., Ivanov, I., Mosin, O. V.* (2015). Studying of Virucidal and Biocidal Effects of Electrochemically Activated Anolyte and Catholyte Types of Water on Classical Swine Fever Virus (CSF) and Bacterium E. coli DH5. *Journal of Medicine, Physiology and Biophysics*, Vol. 13: pp. 1-17.

Ignatov et al., 2015 - *Ignatov, I., Mosin, O.V., Gluhchev, G., Karadzhov, S., Miloshev, G., Ivanov, N.* (2015). The Evaluation of Mathematical Model of Interaction of Electrochemically Activated Water Solutions (Anolyte and Catholyte) with Water. *European Reviews of Chemical Research*, Vol. 2 (4): pp. 72-86.

Ignatov, 2005 – *Ignatov, I.* (2005). Energy Biomedicine. *Gea-Libris, Sofia*, pp. 1–88.

Ignatov, 2010 – Ignatov, I. (2010). Which Water is Optimal for the Origin (Generation) of Life? *Euromedica*, Hanover: 34-35.

Ignatov, 2011 – *Ignatov, I.* (2011). Entropy and Time in Living Matter. *Euromedica:* 74 p.

Ignatov, 2012 – *Ignatov, I.* (2012). Origin of Life and Living Matter in Hot Mineral Water, Conference on the Physics, Chemistry and Biology of Water. *Vermont Photonics*, USA.

Ignatov, Mosin, 2013 – *Ignatov I., Mosin O.V.* (2013). Possible Processes for Origin of Life and Living Matter with Modeling of Physiological Processes of Bacterium *Bacillus Subtilis* in Heavy Water as Model System. *Journal of Natural Sciences Research*, Vol. 3 (9): pp. 65-76.

Ignatov, Mosin, 2013 – *Ignatov, I., Mosin, O. V.* (2013). Modeling of Possible Processes for Origin of Life and Living Matter in Hot Mineral and Seawater with Deuterium. *Journal of Environment and Earth Science*, Vol. 3(14): pp. 103-118.

Ignatov, Mosin, 2014b – *Ignatov, I., Mosin, O. V.* (2014). The Structure and Composition of Carbonaceous Fullerene Containing Mineral Shungite and Microporous Crystalline Aluminosilicate Mineral Zeolite. Mathematical Model of Interaction of Shungite and Zeolite with Water Molecules. *Advances in Physics Theories and Applications*, Vol.28: pp. 10-21.

Ignatov, Mosin, 2014c – *Ignatov, I., Mosin, O.V.* (2014). The Structure and Composition of Shungite and Zeolite. Mathematical Model of Distribution of Hydrogen Bonds of Water Molecules in Solution of Shungite and Zeolite. *Journal of Medicine, Physiology and Biophysics*, Vol. 2: pp. 20-36.

Ignatov, Mosin, 2014d – *Ignatov, I., Mosin, O.V.* (2014). Mathematical Models of Distribution of Water Molecules Regarding Energies of Hydrogen Bonds, *Journal of Medicine, Physiology and Biophysics*, Vol. 2: pp. 71-94.

Ignatov, Mosin, 2014e – *Ignatov, I., Mosin,O.V.* (2014). Mathematical Model of Interaction of Carbonaceous Fullerene Containing Mineral Shungite and Aluminosilicate Mineral Zeolite with Water. *Journal of Medicine, Physiology and Biophysics*, Vol. 3: pp. 15-29.

Ignatov et al., 2014 – *Ignatov, I., Mosin, O. V., Bauer, E.* (2014). Carbonaceous Fullerene Mineral Shungite and Aluminosilicate Mineral Zeolite. Mathematical Model ans Practical Application of Water Solution of Water Shungite and Zeolite. *Journal of Medicine, Physiology and Biophysics*, Vol. 4: pp. 27-44.

Ignatov, Mosin, 2016a – *Ignatov, I., Mosin, O.V.* (2016). Water for Origin of Life. *Altaspera Publishing & Literary Agency Inc.* pp. 1-616. [in Russian]

Ignatov, Mosin, 2016b – Ignatov, I., Mosin, O.V. (2016). Deuterium, Heavy Water and Origin of Life. *LAP LAMBERT Academic Publishing*, pp. 1-500.

Ignatov et al., 2016 – *Ignatov, I. et al.* (2016). Results of Biophysical and Nano Technological Research of ZEOLITH Detox of LavaVitae Company. *Journal of Health, Medicine and Nursing*, Vol. 30, pp. 44-49.

Ignatov, 2006 – *Ignatov, I.* (2016). Product of LavaVitae BOOST is Increasing of Energy of Hydrogen Bonds among Water Molecules in Human Body. *Journal of Medicine, Physiology and Biophysics*, Vol. 27., pp. 30-42.

Ignatov, 2016 – *Ignatov, I.* (2016). VITA intense – Proofs for Anti-inflammatory, Antioxidant and Inhibition Growth of Tumor Cells Effects. Relaxing Effect of Nervous System. Anti Aging Influence. *Journal of Medicine, Physiology and Biophysics*, Vol. 27, pp. 43-61.

Ignatov et al., 2014 – *Ignatov, I., Karadzhov, S., Atanasov, A., Ivanova, E., Mosin, O. V.* (2014). Electrochemical Aqueous Sodium Chloride Solution (Anolyte and Catholyte) as Types of

Water. Mathematical Models. Study of Effects of Anolyte on the Virus of Classical Swine Fever Virus. *Journal of Health, Medicine and Nursing*, Vol. 8: pp. 1-28.

Ignatov et al., 2015a – *Ignatov, I., Gluhchev, G., Karadzhov, S., Miloshev, G., Ivanov, I., Mosin, O.V.* (2015). Preparation of Electrochemically Activated Water Solutions (Catholyte/Anolyte) and Studying Their Physical-Chemical Properties. *Journal of Medicine, Physiology and Biophysics*, Vol. 11: pp. 1-21.

Ignatov et al., 2015b – *Ignatov, I., Gluhchev, G., Karadzhov, S., Miloshev, G., Ivanov, I., Mosin, O. V.* (2015). Preparation of Electrochemically Activated Water Solutions (Catholyte/Anolyte) and Studying of their Physical-Chemical Properties. *Journal of Medicine, Physiology and Biophysics*, Vol. 13, pp. 18-38.

Ignatov et al., 2015c – *Ignatov, I., Gluhchev, G., Karadzhov, S., Miloshev, G., Ivanov, I., Mosin, O. V.* (2015). Preparation of Electrochemically Activated Water Solutions (Catholyte/Anolyte) and Studying of their Physical-Chemical Properties. *Journal of Health, Medicine and Nursing*, Vol. 13: pp. 64-78.

Ignatov et al., 2015d – *Ignatov, I., Mosin, O. V., Gluhchev, G., Karadzhov, S., Miloshev, G., Ivanov, I.* (2015). Studying Electrochemically Activated NaCl Solutions of Anolyte and Catholyte by Methods of Non-Equilibrium Energy Spectrum (NES) and Differential Non-Equilibrium Energy Spectrum (DNES). *Journal of Medicine, Physiology and Biophysics*, Vol. 14: pp. 6-18.

Ignatov et al., 2015e – Ignatov, I, Gluhchev, G., Karadzhov, S., Ivanov, N., Mosin, O.V. (2015). Preparation of Electrochemically Activated Water Solutions (Catholyte/Anolyte) and Studying Their Physical-Chemical Properties. *Journal of Medicine, Physiology and Biophysics*, Vol. 16: pp. 1-14.

Ignatov et al., 2016 – *Ignatov, I., Mosin, O.V., Gluhchev, G., Karadzhov, S., Miloshev, G., Ivanov, I.* (2016). Studying Electrochemically Activated NaCl Solutions of Anolyte and Catholyte by Methods of Non-Equilibrium Energy Spectrum (NES) and Differential Non-Equilibrium Energy Spectrum (DNES). *Journal of Medicine, Physiology and Biophysics*, Vol. 20: pp. 13-23.

Ignatov, 2017 – *Ignatov, I.* (2017). Aluminosilicate Mineral Zeolite. Interaction of Water Molecules in Zeolite Table and Mountain Water Sevtopolis from Bulgaria. *Journal of Medicine, Physiology and Biophysics*, Vol. 31, pp. 41-45.

Ignatov, Mosin, 2015 – *Ignatov, I., Mosin O.V.* (2015). Origin of Life and Living Matter in Hot Mineral Water. *Advances in Physics Theories and Applications*, Vol. 39: 1-22.

Ignatov, 2017 – *Ignatov, I.* (2017). VITA intense and Boost – Products with Natural Vitamins and Minerals for Health. *Journal of Medicine, Physiology and Biophysics*, Vol. 31, pp. 58-78.

Ignatov, 2017 – *Ignatov, I.* (2017). ZEOLITH detox for Detoxification and ZELOLITH Creme for Skin Effects as Products of LavaVitaae Company. *Journal of Medicine, Physiology and Biophysics,* Vol. 31, pp. 79-86.

Ignatov, Mosin, 2014a – *Ignatov, I., Mosin, O.V.* (2014). Methods for Measurements of Water Spectrum. Differential Non-equilibrium Energy Spectrum Method (DNES). *Journal of Health, Medicine and Nursing,* Vol. 6, pp. 50-72.

Ignatov, Mosin, 2014b – *Ignatov, I., Mosin, O.V.* (2014). Mathematical Models of Distribution of Water Molecules Regarding Energies of Hydrogen Bonds. *Journal of Medicine, Physiology and Biophysics,* Vol. 6, pp. 50-72.

Ignatov, Mosin, 2014c – *Ignatov, I., Mosin, O.V.* (2014). Structural Models of Water and Ice Regarding the Energy of Hydrogen Bonding. *Nanotechnology Research and Practice*, Vol. 7 (3): pp. 96-117.

Ignatov, 2017 – *Ignatov, I.* (2017). VITA intense and Boost – Products with Natural Vitamins and Minerals for Health. *Journal of Medicine, Physiology and Biophysics*, Vol. 31, pp. 58-78.

Ignatov, 2017 – *Ignatov, I.* (2017). ZEOLITH detox for Detoxification and ZELOLITH Creme for Skin Effects as Products of LavaVitaae Company. *Journal of Medicine, Physiology and Biophysics,* Vol. 31, pp. 79-86.

Ignatov, Mosin, 2014a – *Ignatov, I., Mosin, O.V.* (2014). Methods for Measurements of Water Spectrum. Differential Non-equilibrium Energy Spectrum Method (DNES). *Journal of Health, Medicine and Nursing,* Vol. 6, pp. 50-72.

Ignatov, Mosin, 2015 – *Ignatov, I., Mosin O.V.* (2015). Origin of Life and Living Matter in Hot Mineral Water. *Advances in Physics Theories and Applications*, Vol. 39: 1-22.

Ignatov, Mosin, 2014b – *Ignatov, I., Mosin, O.V.* (2014). Mathematical Models of

Distribution of Water Molecules Regarding Energies of Hydrogen Bonds. *Journal of Medicine, Physiology and Biophysics,* Vol. 6, pp. 50-72.

Ignatov, Mosin, 2014c – *Ignatov, I., Mosin, O.V.* (2014). Structural Models of Water and Ice Regarding the Energy of Hydrogen Bonding. *Nanotechnology Research and Practice*, Vol. 7 (3): pp. 96-117.

Ignatov, Mosin, 2014d – *Ignatov, I., Mosin, O.V.* (2014). Nano Mix of Shungite and Zeolite for Cleaning of Toxins and Increasing of Energy of Hydrogen Bonds among Water Molecules in Human Body. *Journal of Medicine, Physiology and Biophysics,* Vol. 27, pp. 1-10.

Luck et al., 1980 – *Luck, W., Schiöberg, D., Ulrich, S.* (1980). Infared Investigation of Water Structure in Desalination Membranes. *J. Chem. Soc. Faraday Trans.*, Vol. 2(76), pp. 136–147.

Mehandjiev et al., 2017 – *Mehandjiev, D., Ignatov, I., Karadzhov, I., Gluhchev, G., Atanasov, A.* (2017). On the Mechanism of Water Electrolysis. *Journal of Medicine, Physiology and Biophysics,* Vol. 31, pp. 23-26.

Mosin, Ignatov, 2013 – *Mosin, O.V., Ignatov, I.* (2013). The Structure and Composition of Natural Carbonaceous Fullerene Containing Mineral Shungite. *International Journal of Advanced Scientific and Technical Research*, Vol. 6(11–12), pp. 9–21.

Mosin, Ignatov, 2012a – *Mosin, O.V., Ignatov, I.* (2012). The Composition and Structural Properties of Fullerene Natural Mineral Shungite. *Nanoengineering*, Vol. 18 (12), pp. 17–24 [in Russian]

Mosin, Ignatov, 2012b – *Mosin, O.V., Ignatov, I.* (2012). Composition and Structural Properties of Fullerene Natural Mineral Shungite. *Nanomaterials and Nanotechnologies,* 2: pp. 25-36.

Mosin, Ignatov, 2015 – *Mosin, O.V., Ignatov, I.* (2015). An Overview of Methods and Approaches for Magnetic Treatment of Water. *Water: Hygiene and Ecology*, Vol. 3-4 (4): pp. 113-130.

Panayotova, Velikov, 2002 – *Panayotova, M., Velikov, B.* (2002). Kinetics of heavy metal ions removal by use of natural zeolite. *Journal of Environmental Science and Health*, *Vol.* 37(2): pp. 139–147.

Parfen'eva, 1994 – *Parfen'eva, L.S.* (1994). Electrical Conductivity of Shungite Carbon. *Solid State Physics*, *Vol.* 36(1), pp. 234–236.

Podchaynov, 2007 – *Podchaynov, S.F.* (2007). Mineral zeolite – a multiplier of useful properties shungite. Shungites and human safety. *Proceedings of the First All-Russian scientific-practical conference* (3–5 October 2006), ed. J.K Kalinin (Petrozavodsk: Karelian Research Centre of Russian Academy of Sciences), pp/ 6–74 [in Russian]

Copyright © 2017 by Academic Publishing House Researcher s.r.o.

Published in the Slovak Republic
European Journal of Molecular Biotechnology
Has been issued since 2013.
ISSN: 2310-6255
E-ISSN: 2409-1332
2017, 5(1): 23-29

DOI: 10.13187/ejmb.2017.1.23
www.ejournal8.com

Processes in Catholyte and Anolyte as Result of Water Electrolysis

Dimitar Mehandjiev [a], Ignat Ignatov [b, *], Stoil Karadzhov [c], Georgi Gluhchev [d], Atanas Atanasov [e]

[a] Institute of General and Inorganic Chemistry, Bulgarian Academy of Science (BAS), Acad. G. Bonchev Street, Sofia, Bulgaria
[b] Scientific Research Center of Medical Biophysics (SRCMB), Bulgaria
[c] Bulgarian Association of Activated Water, Sofia, Bulgaria
[d]. Institute of Information and Communication Technologies (BAS), Sofia, Bulgaria
[e] Bulgarian Association of Activated Water, Sofia, Bulgaria

Abstract

A two stage model of the physicochemical processes at the electrolysis of pure water is proposed. The presence of nascent hydrogen in the catholyte and nascent oxygen in the anolyte during the first stage explains the antioxidant properties of the catholyte and the strong biocidal action of the anolyte. In the second stage the nascent hydrogen and oxygen are combined into hydrogen and oxygen molecules, respectively. The comparison between their average energies with the average energy of the control sample of water shows an increase in the average energy of the catholyte and decrease in the average energy of the anolyte. This indicates that some changes in the structure of the activated water have occurred.

Keywords: Electrochemically activated water (ECAW), catholyte, anolyte, nascent hydrogen, nascent oxygen, energetic spectrum, energy of hydrogen bonds.

2. Introduction

Water is the main factor of the life on our planet. Even more, according to one of the co-authors of this paper the life has started in the warm thermal springs on the earth (Ignatov, Mosin, 2015). Water regulates the vital processes in the living things actively participating in the metabolism and their adaptation to the environment. That's why every change of its composition and structure influences the live matter either aiding its development and stability or on contrary provoking its destruction. It seems strange that despite such enormous importance scientists from different countries have seriously started paying attention and investigating the unusual properties of the water put to different kind of influence only in the last decades. In this direction a great attention was paid to its electrochemical activation (Bakhir, 1999; Kloss, 1988; Petrushenko, Lobyshev, 2004; Prilutsky, Bakhir, 1997; Zenin, 1999). Notwithstanding the easy description of the chemical processes the explanation of the obtained properties of the alkaline (catholyte) and acidic (anolyte) water solutions are still not fully convincing (Ball, 2008). Even more, in the majority of the existing descriptions and experiments NaCl has been used which gives a satisfactory explanation of the biocidal properties of the anolyte but does not work in case of pure water which obtains same properties. The explanation probably relates not only to the chemical changes in the water composition but also to the changes of its structure.

* Corresponding author
E-mail addresses: mbioph@dir.bg (I. Ignatov)

The main questions that researchers have to answer are as follows.

1. What physical and chemical changes occur in the water during its electrolysis?

This question should be investigated in two aspects:

а) pure water is processed;

б) NaCl or other minerals are added to the water solution.

2. What parameters of the activated water play a major role for the explanation of its unusual properties?

3. What the mechanism of the action of the activated water on the living things is?

In this paper attention is paid to the question 1a), i.e. the activation of water without additional mineralization, free of ions of other elements. A model of the corresponding physicochemical processes is proposed.

Every model has to describe satisfactory the observed effects of the modeled process. In our case the known effects of the activated water (catholyte and anolyte) reported by different investigators concern especially its influence on the living things. An explanation for the described effects could be the increased presence of both molecular hydrogen (H_2) in the catholyte solution and molecular oxygen (O_2) in the anolyte solution. But such an increase can be achieved through saturation of the water solution with these gases as well. It is true that in this case the water properties will be changed but without same effects. It is reasonable to assume that the increased concentration of OH^- ions in the catholyte as well as H^+ ions in the anolyte cause such an action. Therefore, one may conclude **that the action of the direct current on distilled or de-ionized water leads to changes in its chemical composition and structure different for the catholyte and anolyte.**

Electrolysis of pure water.

According to the modern notion the following reaction takes place at the cathode :

$$2H^+ + 2e^- \rightarrow H_2\uparrow \quad (1)$$

The analogous reaction at the anode is as follows:

$$2O^{2-} - 2e^- \rightarrow O_2\uparrow \quad (2)$$

Actually, the above reactions run in two stages.

At the cathode:

First stage $H^+ + e^- \rightarrow H^*$ (3)

Second stage $H^* + H^* \rightarrow H_2$ (4)

At the anode:

First stage $OH \rightarrow O^* + 2e^- + H^+$ (5)

Second stage $O^* + O^* \rightarrow O_2$ (6)

Therefore, according to formula (3) H^* - atomic hydrogen is produced at the cathode during the first stage. It is called also nascent hydrogen and possesses high reactivity. Atomic oxygen O^* called also nascent oxygen is produced at the anode, and it is highly reactive as well. These atoms can react between them according to formulae (4) and (6), and the obtained hydrogen and oxygen molecules can be either separated from the solution and go to the air or remain dissolved in the water. If there are molecules of hydrogen and oxygen at the cathode and the anode obtained according to formulae (4) и (6) they can react with the nascent hydrogen and oxygen respectively as follows:

$$4H^* + O_2 \rightarrow 2H_2O \quad (7)$$

$$O^* + H_2 \rightarrow H_2O \quad (8)$$

and water molecules will be produced.

2. Results and Discussion

It is supposed in the proposed model that nascent hydrogen and nascent oxygen are produced in the catholyte and anolyte respectively. Their presence is substantial for the processes that may occur in the above solutions. The most probable assumption is that they will take part in reactions (4) and (6) or for example (7) and (8). Another possibility for them is to be stabilized in small quantity. It has to be underlined that the stabilization possibility depends on the probability to encounter corresponding re-agents from the above mentioned reactions. If this probability is small there is a possibility other molecules that can not react with them to play the role of

stabilizers. For example, the water molecules due to their dipole character allowing for the formation of dimmers, thrimmers and larger structures could play such a role. In that case stabilized atoms of nascent hydrogen will remain in the catholyte, and stabilized atoms of nascent oxygen will remain in the anolyte. Since the nascent hydrogen is an active reducer it will attack admixtures that could be reduced when the catholyte is blended with another medium. This could explain the catholyte action as a strong antioxidant (Hanaoka, 2001; Kokichi et al., 2004). Probably, this could explain its healthy influence in case of different stress-related or due to the action of free radicals deceases. Such influence has been observed by many researchers (Hayashi, Kawamura, 2002; Komatsu et al., 2001; Lee et al., 2006; Sanetaka Shirahata et al., 2012; Yahagi,et al., 2000; Ye et al., 2008; Ye, Jun et al., 2004).

In a similar way the anolyte put in another medium will demonstrate its strong oxidative property and will oxidize all present organic admixtures and will destroy microorganisms, bacteria and viruses (Gluhchev et al., 2015; Karadzov et al., 2014; Kirkpatrick, 2009; Kumar et al., 1999; Miroshnikov, 2002; Suzuki et al., 2002; Tanaka et al., 1996; Zinkevich et al., 2000), which makes it an excellent biocidal, disinfection and harmless for the people and the environment mean.

The presence of nascent hydrogen and nascent oxygen in the hydrolyzed water could produce changes in its state. Indeed, using the method NES (Antonov, 1995; Ignatov, Mosin, 2014) as a measure of the energy spectrum of the water stage a useful information could be obtained about the structural changes in water and the average energy of hydrogen bonds among individual H_2O molecules in samples. It was experimentally established (Ignatov, Mosin, 2014) that the surface pressure was increased in the catholyte and more molecules were included in a unit volume. The average energy E of the hydrogen bonds H...O between water molecules H_2O, measured for the catholyte and anolyte, accordingly when a de-ionized water is used is E = -0.1293 eV for the catholyte and E = -1221 eV for the anolyte. The difference $\Delta E_{H...O}$ between the average energy of the control sample of water E = -0.1251 eV, evaluated by the method DNES (Ignatov, Mosin, 2014) and the average energy of the catholyte and anolyte is respectively ΔE= -0.0042 ± 0.0011 eV and ΔE= 0.003 ± 0.0011 eV.

4. Discussion and Conclusions

A two-stage model describing physicochemical processes stemming from the electrolysis of pure water is suggested in the paper. The production of nascent hydrogen and nascent oxygen during the first stage is used as a basic assumption. The enriched concentration of these components in the solutions explains the antioxidant action of the catholyte the strong biocidal effect of the anolyte. The observed difference in the average energy and hydrogen bonds between catholyte and anolyte is an indication of structural changes that have taken place in the activated water. The development of more general model describing the physicochemical processes and analysis of the content and structure of activated water in case of electrolysis of weak water mineralization is a subject of future work.

References

Antonov, 1995 – *Antonov, A.* (1995). Research of the Nonequilibrium Processes in the Area in Allocated Systems. *Diss. Thesis Doctor of Physical Sciences. Sofia*: *Blagoevgrad*: pp. 1–255.

Bakhir, 1999 – *Bakhir, V.M.* (1999). Theoretical Aspects of Electrochemical Activation. *2nd Int. Conf. Electrochemical Actvation in Medicine, Agriculture and Industry.* [in Russian]

Ball, 2008 – *Ball, P.* (2008). Water – an Enduring Mystery. *Nature,* Vol. 452*:* 20 p.

Dimitrova et al., 2015 – *Dimitrova, L., Kussovski, V., Tsvetkova, I., Mihaylova, S., Ivanov, N., Gluhchev, G., Najdenski, H.* (2015). Bacterial Effect of Electrochemically Activated Water on the Aerobic Bacterial Population on Digestate. *Ecological Engineering and Environment Protection*, Vol. 4, 23-32 [in Bulgarian]

Gluhchev et al., 2015a – *Gnluhchev, G., Ignatov, I., Karadzhov, S., Miloshev, G., Ivanov, I., Mosin, O.V.* (2015). Biocidal Effects of Electrochemically Activated Water. *Journal of Health, Medicine and Nursing*, V. 11: pp. 67-83.

Gluhchev et al., 2015b – *Gluhchev, G., Ignatov, I., Karadzhov, S., Miloshev, G., Ivanov, N., Mosin, O.V.* (2015). Electrochemically Activited Water: Biophysical and Biological Effects of Anolyte and Catholyte Types of Water. *European Journal of Molecular Biotechnology*, V.1, pp. 12-26.

Gluhchev et al., 2015c – *Gluhchev, G., Ignatov, I., Karadzhov, S., Miloshev, G., Ivanov, N.,*

Mosin, O.V. (2015). Studying the Antimicrobial and Antiviral Effects of Electrochemically Activated Nacl Solutions of Anolyte and Catholyte on a Strain of E. Coli DH5 and Classical Swine Fever (CSF) Virus. *European Journal of Medicine*, 9 (3): pp. 124-138.

Gluhchev et al., 2015d – *Gluhchev, G., Ignatov, I., Karadzhov, S., Miloshev, G., Ivanov, I., Mosin, O.V.* (2015). Electrochemically Activated Water. Biophysical and Biological Effects of Anolyte and Catholyte as Types of Water. *Journal of Medicine, Physiology and Biophysics*, Vol. 10: pp. 1-17.

Gluhchev et al., 2015e – *Gluhchev, G., Ignatov, I., Karadzhov, S., Miloshev, G., Ivanov, I., Mosin, O. V.* (2015). Studying of Virucidal and Biocidal Effects of Electrochemically Activated Anolyte and Catholyte Types of Water on Classical Swine Fever Virus (CSF) and Bacterium E. coli DH5. *Journal of Medicine, Physiology and Biophysics*, Vol. 13: pp. 1-17.

Hanaoka, 2001 – *Hanaoka, K.* (2001). Antioxidant Effects of Reduced Water Produced by Electrolysis of Sodium Chloride solutions. *Journal of Applied Electrochemistry*, Vol. 31: pp. 1307–1313.

Hayashi, Kawamura, 2002 – *Hayashi, H., Kawamura, M.* (2002). Clinical Application of Electrolyzed-reduced Water. In S. Shirahata et al. (Eds). *Animal cell technology: Basic and applied aspects,* Vol. 12: pp. 31-36.

Ignatov et al., 2015 – *Ignatov, I., Mosin, O.V., Gluhchev, G., Karadzhov, S., Miloshev, G., Ivanov, N.* (2015). The Evaluation of Mathematical Model of Interaction of Electrochemically Activated Water Solutions (Anolyte and Catholyte) with Water. *European Reviews of Chemical Research*, Vol. 2 (4): pp. 72-86.

Ignatov, 2005 – *Ignatov, I.* (2005). Energy Biomedicine. *Gea-Libris, Sofia*, pp. 1–88.

Ignatov, 2010 – Ignatov, I. (2010). Which Water is Optimal for the Origin (Generation) of Life? *Euromedica*, Hanover: 34-35.

Ignatov, 2011 – *Ignatov, I.* (2011). Entropy and Time in Living Matter. *Euromedica:* 74 p.

Ignatov, 2012 – *Ignatov, I.* (2012). Origin of Life and Living Matter in Hot Mineral Water, Conference on the Physics, Chemistry and Biology of Water. *Vermont Photonics*, USA.

Ignatov, Mosin, 2013 – *Ignatov I., Mosin O.V.* (2013). Possible Processes for Origin of Life and Living Matter with Modeling of Physiological Processes of Bacterium *Bacillus Subtilis* in Heavy Water as Model System. *Journal of Natural Sciences Research*, Vol. 3 (9): pp. 65-76.

Ignatov, Mosin, 2013 – *Ignatov, I., Mosin, O. V.* (2013). Modeling of Possible Processes for Origin of Life and Living Matter in Hot Mineral and Seawater with Deuterium. *Journal of Environment and Earth Science*, Vol. 3(14): pp. 103-118.

Ignatov, Mosin, 2013 – *Ignatov, I., Mosin, O. V.* (2013). Structural Mathematical Models Describing Water Clusters. *Journal of Mathematical Theory and Modeling*, Vol.3 (11): pp. 72-87.

Ignatov, Mosin, 2014a – *Ignatov, I., Mosin, O. V.* (2014). Nature of Haydrogen Bonds in Liquids and Crystals. Ice Crystal Modifications and Their Physical Characteristics. *Journal of Medicine, Physiology and Biophysics*, Vol. 4: pp. 58-80.

Ignatov, Mosin, 2014b – *Ignatov, I., Mosin, O. V.* (2014). The Structure and Composition of Carbonaceous Fullerene Containing Mineral Shungite and Microporous Crystalline Aluminosilicate Mineral Zeolite. Mathematical Model of Interaction of Shungite and Zeolite with Water Molecules. *Advances in Physics Theories and Applications*, Vol.28: pp. 10-21.

Ignatov, Mosin, 2014c – *Ignatov, I., Mosin, O.V.* (2014). The Structure and Composition of Shungite and Zeolite. Mathematical Model of Distribution of Hydrogen Bonds of Water Molecules in Solution of Shungite and Zeolite. *Journal of Medicine, Physiology and Biophysics*, Vol. 2: pp. 20-36.

Ignatov, Mosin, 2014d – *Ignatov, I., Mosin, O.V.* (2014). Mathematical Models of Distribution of Water Molecules Regarding Energies of Hydrogen Bonds, *Journal of Medicine, Physiology and Biophysics*, Vol. 2: pp. 71-94.

Ignatov, Mosin, 2014e – *Ignatov, I., Mosin,O.V.* (2014). Mathematical Model of Interaction of Carbonaceous Fullerene Containing Mineral Shungite and Aluminosilicate Mineral Zeolite with Water. *Journal of Medicine, Physiology and Biophysics*, Vol. 3: pp. 15-29.

Ignatov et al., 2014 – *Ignatov, I., Mosin, O. V., Bauer, E.* (2014). Carbonaceous Fullerene Mineral Shungite and Aluminosilicate Mineral Zeolite. Mathematical Model ans Practical Application of Water Solution of Water Shungite and Zeolite. *Journal of Medicine, Physiology and Biophysics*, Vol. 4: pp. 27-44.

Ignatov, Mosin, 2016a – *Ignatov, I., Mosin, O.V.* (2016). Water for Origin of Life. *Altaspera Publishing & Literary Agency Inc.* pp. 1-616. [in Russian]

Ignatov, Mosin, 2016b – Ignatov, I., Mosin, O.V. (2016). Deuterium, Heavy Water and Origin of Life. *LAP LAMBERT Academic Publishing*, pp. 1-500.

Ignatov et al., 2016 – *Ignatov, I. et al.* (2016). Results of Biophysical and Nano Technological Research of ZEOLITH Detox of LavaVitae Company. *Journal of Health, Medicine and Nursing*, Vol. 30, pp. 44-49.

Ignatov, 2006 – *Ignatov, I.* (2016). Product of LavaVitae BOOST is Increasing of Energy of Hydrogen Bonds among Water Molecules in Human Body. *Journal of Medicine, Physiology and Biophysics*, Vol. 27., pp. 30-42.

Ignatov, 2016 – *Ignatov, I.* (2016). VITA intense – Proofs for Anti-inflammatory, Antioxidant and Inhibition Growth of Tumor Cells Effects. Relaxing Effect of Nervous System. Anti Aging Influence. *Journal of Medicine, Physiology and Biophysics*, Vol. 27, pp. 43-61.

Ignatov et al., 2014 – *Ignatov, I., Karadzhov, S., Atanasov, A., Ivanova, E., Mosin, O. V.* (2014). Electrochemical Aqueous Sodium Chloride Solution (Anolyte and Catholyte) as Types of Water. Mathematical Models. Study of Effects of Anolyte on the Virus of Classical Swine Fever Virus. *Journal of Health, Medicine and Nursing*, Vol. 8: pp. 1-28.

Ignatov et al., 2015a – *Ignatov, I., Gluhchev, G., Karadzhov, S., Miloshev, G., Ivanov, I., Mosin, O.V.* (2015). Preparation of Electrochemically Activated Water Solutions (Catholyte/Anolyte) and Studying Their Physical-Chemical Properties. *Journal of Medicine, Physiology and Biophysics*, Vol. 11: pp. 1-21.

Ignatov et al., 2015b – *Ignatov, I., Gluhchev, G., Karadzhov, S., Miloshev, G., Ivanov, I., Mosin, O. V.* (2015). Preparation of Electrochemically Activated Water Solutions (Catholyte/Anolyte) and Studying of their Physical-Chemical Properties. *Journal of Medicine, Physiology and Biophysics*, Vol. 13, pp. 18-38.

Ignatov et al., 2015c – *Ignatov, I., Gluhchev, G., Karadzhov, S., Miloshev, G., Ivanov, I., Mosin, O. V.* (2015). Preparation of Electrochemically Activated Water Solutions (Catholyte/Anolyte) and Studying of their Physical-Chemical Properties. *Journal of Health, Medicine and Nursing*, Vol. 13: pp. 64-78.

Ignatov et al., 2015d – *Ignatov, I., Mosin, O. V., Gluhchev, G., Karadzhov, S., Miloshev, G., Ivanov, I.* (2015). Studying Electrochemically Activated NaCl Solutions of Anolyte and Catholyte by Methods of Non-Equilibrium Energy Spectrum (NES) and Differential Non-Equilibrium Energy Spectrum (DNES). *Journal of Medicine, Physiology and Biophysics*, Vol. 14: pp. 6-18.

Ignatov et al., 2015e – Ignatov, I, Gluhchev, G., Karadzhov, S., Ivanov, N., Mosin, O.V. (2015). Preparation of Electrochemically Activated Water Solutions (Catholyte/Anolyte) and Studying Their Physical-Chemical Properties. *Journal of Medicine, Physiology and Biophysics*, Vol. 16: pp. 1-14.

Ignatov et al., 2016 – *Ignatov, I., Mosin, O.V., Gluhchev, G., Karadzhov, S., Miloshev, G., Ivanov, I.* (2016). Studying Electrochemically Activated NaCl Solutions of Anolyte and Catholyte by Methods of Non-Equilibrium Energy Spectrum (NES) and Differential Non-Equilibrium Energy Spectrum (DNES). *Journal of Medicine, Physiology and Biophysics*, Vol. 20: pp. 13-23.

Ignatov, 2017 – *Ignatov, I.* (2017). Aluminosilicate Mineral Zeolite. Interaction of Water Molecules in Zeolite Table and Mountain Water Sevtopolis from Bulgaria. *Journal of Medicine, Physiology and Biophysics*, Vol. 31, pp. 41-45.

Ignatov, Mosin, 2015 – *Ignatov, I., Mosin O.V.* (2015). Origin of Life and Living Matter in Hot Mineral Water. *Advances in Physics Theories and Applications*, Vol. 39: 1-22.

Ignatov, 2017 – *Ignatov, I.* (2017). VITA intense and Boost – Products with Natural Vitamins and Minerals for Health. *Journal of Medicine, Physiology and Biophysics*, Vol. 31, pp. 58-78.

Ignatov, 2017 – *Ignatov, I.* (2017). ZEOLITH detox for Detoxification and ZELOLITH Creme for Skin Effects as Products of LavaVitaae Company. *Journal of Medicine, Physiology and Biophysics,* Vol. 31, pp. 79-86.

Ignatov, Mosin, 2014a – *Ignatov, I., Mosin, O.V.* (2014). Methods for Measurements of Water Spectrum. Differential Non-equilibrium Energy Spectrum Method (DNES). *Journal of Health, Medicine and Nursing,* Vol. 6, pp. 50-72.

Ignatov, Mosin, 2014b – *Ignatov, I., Mosin, O.V.* (2014). Mathematical Models of Distribution of Water Molecules Regarding Energies of Hydrogen Bonds. *Journal of Medicine,*

Physiology and Biophysics, Vol. 6, pp. 50-72.

Ignatov, Mosin, 2014c – *Ignatov, I., Mosin, O.V.* (2014). Structural Models of Water and Ice Regarding the Energy of Hydrogen Bonding. *Nanotechnology Research and Practice*, Vol. 7 (3): pp. 96-117.

Ignatov, Mosin, 2014d – *Ignatov, I., Mosin, O.V.* (2014). Nano Mix of Shungite and Zeolite for Cleaning of Toxins and Increasing of Energy of Hydrogen Bonds among Water Molecules in Human Body. *Journal of Medicine, Physiology and Biophysics,* Vol. 27, pp. 1-10.

Luck et al., 1980 – *Luck, W., Schiöberg, D., Ulrich, S.* (1980). Infared Investigation of Water Structure in Desalination Membranes. *J. Chem. Soc. Faraday Trans.*, Vol. 2(76), pp. 136–147.

Kirkpatrick, 2009 – *Kirkpatrick, R. D.* (2009). The Mechanism of Antimicrobial Action of Electro-chemically Activated (ECA) Water and its Healthcare Applications", *Doctoral Thesis, University of Pretoria.*

Kloss, 1988 – *Kloss, A.I.* (1988). Electron-radical Dissociation and Mechanism of Water Activation. *Trans. Acad. Sc. USSR,* Vol. 303: pp. 1403-1406. [in Russian]

Kokichi et al., 2004 – *Kokichi H., Dongxu S., R., Lawrence, Y. Kamitani, Fernandes G.* (2004). The Mechanism of the Enhanced Antioxidant Effects Against Superoxide Anion Radicals of Reduced Water Produced by Electrolysis. *Biophisical Chemistry,* Vol. 107: pp. 71-82.

Komatsu et al., 2001 – *Komatsu, T., Kabayama, S., Hayashida, A et al.* (2001). Suppressive Effect of Electrolyzed Reduced Water on the Growth of Cancer Cells and Microorganisms. *In E. Lindner-Olsson, N.* Chatzissavidou, L. Elke (Eds). Animal cell technology: From target to market. Dordrecht://*Kluwer Academic Publishers*. pp. 220-223

Kumar et al., 1999 – *Kumar, S. V., Ezeike, G. O., Hung, Y-C., Doyle, M. P.* (1999). Efficacy of Electrolyzed Oxidizing Water for Inactivating Escherhia coli O157:H7, Salmonela enteritidis, and Lusteria monocytogenes. *Applied and Evironmental Microbiology*: 4276-4279.

Lee et al., 2004 – Kyu-Jae Lee, Seung-Kyu, Jae-Won, Gwang-Young et al. (2004). Anticancer Effect of Alkaline Water, Korea.

Lee et al., 2006 – *Lee, M-Y., Kim.-K., Ryoo, K.-K et al.* (2006). Electrolyzed-reduced water protects against oxidative damage to DNA, RNA and protein. *Applied Biochemistry and Biotechnology* Vol. 135, pp. 133-144.

Miroshnikov, 2002 – *Miroshnikov, A.I.* (2002). Stimulation and Inhibition of Escherichia coli Cell Growth During Cultivation in the Catholyte and Anolyte of Culture Medium. **Biofizika.** Mar-Apr; Vol. 47(2):pp.304-308. [in Russian]

Mehandjiev et al., 2017 – *Mehandjiev, D., Ignatov, I., Karadzhov, I., Gluhchev, G., Atanasov, A.* (2017). On the Mechanism of Water Electrolysis. *Journal of Medicine, Physiology and Biophysics,* Vol. 31, pp. 23-26.

Mosin, Ignatov, 2013 – *Mosin, O.V., Ignatov, I.* (2013). The Structure and Composition of Natural Carbonaceous Fullerene Containing Mineral Shungite. *International Journal of Advanced Scientific and Technical Research*, Vol. 6(11–12), pp. 9–21.

Mosin, Ignatov, 2012a – *Mosin, O.V., Ignatov, I.* (2012). The Composition and Structural Properties of Fullerene Natural Mineral Shungite. *Nanoengineering*, Vol. 18 (12), pp. 17–24 [in Russian]

Mosin, Ignatov, 2012b – *Mosin, O.V., Ignatov, I.* (2012). Composition and Structural Properties of Fullerene Natural Mineral Shungite. *Nanomaterials and Nanotechnologies,* 2: pp. 25-36.

Mosin, Ignatov, 2015 – *Mosin, O.V., Ignatov, I.* (2015). An Overview of Methods and Approaches for Magnetic Treatment of Water. *Water: Hygiene and Ecology*, Vol. 3-4 (4): pp. 113-130.

Panayotova, Velikov, 2002 – *Panayotova, M., Velikov, B.* (2002). Kinetics of heavy metal ions removal by use of natural zeolite. *Journal of Environmental Science and Health*, *Vol.* 37(2): pp. 139–147.

Parfen'eva, 1994 – *Parfen'eva, L.S.* (1994). Electrical Conductivity of Shungite Carbon. *Solid State Physics*, *Vol.* 36(1), pp. 234–236.

Podchaynov, 2007 – *Podchaynov, S.F.* (2007). Mineral zeolite – a multiplier of useful properties shungite. Shungites and human safety. *Proceedings of the First All-Russian scientific-practical conference* (3–5 October 2006), ed. J.K Kalinin (Petrozavodsk: Karelian Research Centre of Russian Academy of Sciences), pp/ 6–74 [in Russian]

Petrushenko, Lobyshev, 2004 – *Petrushenko I., Lobyshev V.I.* (2004). Physico-chemical

Properties of Aqueous Solutions, Prepared in a Membrane Electrilyzer. *Biofizika, Vol.*49(1): pp. 22-31.

Prilutsky, Bakhir, 1997 – *Prilutsky, V. I., Bakhir V. M.* (1997). Electrochemically Activated Water: Anomalous Properties, Mechanism of Biological Action. *All Russian Scientific Research and Experimental Institude of Medical Engineering* (VNIIIMT), 1: 124. [in Russian]

Shirahata et al., 2012 – *Sanetaka Shirahata, Takeki Hamasaki, Kiishiro Teruya* (2012). Advanced Research on the Health Benefit of Reduced Water. *Trends in Food Science & Technology Vol.* 23: pp. 124-131.

Suzuki et al., 2002 – *Suzuki, T., Itakura, J., Watanabe, M., Ohta, M., Sato, Y., Yamata, Y.* (2002). Inactivation of Staphylococcal Enterotoxin-A with an Electrolyzed Anodic Solution. *Journal of Agricultural and Food Chemistry,* Vol. 50: pp. 230-234.

Tanaka et al., 1996 – *Tanaka, H., Hirakata, Y., Kaku, M., Yoshida, R., Takemura, H,. Mizukane, R.* (1996). Antimicrobial Activity of Superoxidized Water. *Journal of Hospital Infection,* Vol. 34(1): pp. 43-49.

Yahagi et al., 2000 – *Yahagi N., Kono M., Kitahara M., Ohmura A., Sumita O., Hashimoto T.* (2000). Effect of Electrolyzed Water on Wound Healing. *Artificial Organs,* Vol. 24(12): pp. 984-987.

Ye et al., 2008 – *Ye, J., Li, Y., Hamasaki, T., N., Komatsu, E. et al.* (2008). Inhibitory Effect of Electrolyzed Reduced Water on Tumor Angiogenesis. *Biological and Pharmaceutical Bulletin,* Vol. 31: pp. 19-26.

Ye et al., 2004 – *Ye, Jun, K. Teruya, Y. Katakura et al.* (2004). Suppression of Invasion of Cancer Cells and Angiogenesis by Electrolyzed Reduced Water. *World Congress on in Vitro Biology*.

Zenin, 1999 – *Zenin, S. V.* (1999). On the Mechanism of Water Activation, Second Int. Symposium. *Electrochemical Activation in Medicine, Agriculture and Industry*, pp. 155-156 [in Russian]

Zinkevich et al., 2000 – *Zinkevich, V., Beech, I.B., Tapper, R.C., Bogdarina, I.* (2000). The Effect of Super-oxidized Water on Escherichia Coli. *Journal of Hospital Infection*. Vol. 46(2): pp. 153-156.

Copyright © 2017 by Academic Publishing House Researcher s.r.o.

Published in the Slovak Republic
European Journal of Molecular Biotechnology
Has been issued since 2013.
ISSN: 2310-6255
E-ISSN: 2409-1332
2017, 5(1): 30-42

DOI: 10.13187/ejmb.2017.1.30
www.ejournal8.com

Synthesis, Spectral Sensitization, Solvatochromic and Halochromic Evaluation of New Monomethine and Trimethine Cyanine Dyes

H.A. Shindy [a, *], A.K. Khalafalla [a], M.M. Goma [a], A.H. Eed [a]

[a] Department of Chemistry, Faculty of Science, Aswan University, Aswan 81528, Egypt

Abstract

New heterocyclic starting material namely 4,5-dimethyl-2,7-diphenyl-furo[(3,2-d), (3, 2 -d)] bis pyrazole were prepared and employed to synthesis of some novel monomethine cyanine dyes (simple cyanine dyes) and trimethine cyanine dyes (carbocyanine dyes). Spectral sensitization evaluation for all the synthesized cyanine dyes was carried out through investigating their electronic visible absorption spectra in 95% ethanol solution. Solvatochromic and/or hachromic evaluation for some selected dyes were carried out through examining their electronic visible absorption spectra in pure solvents having different polarities [Water (78.54), Dimethylformamide (36.70), Ethanol (24.3), Chloroform (4.806), Carbontetrachloride (2.238) and Dioxane (2.209)] and/or in aqueous universal buffer solutions having varied pH values (1.75, 2.45, 4.65, 5.80, 7.88, 8.75, 10.85 and 12.60 units), respectively. Structure determination were carried out via elemental analysis, visible spectra. Mass spectrometer, IR and ^{1}H NMR spectral data.

Keywords: Synthesis, cyanine dyes, visible spectra, halochromism, solvatochromism, carbocyanine dyes.

1. Introduction

Increased research interest in cyanine dyes chemistry (Shindy et al., 2012, Shindy et al, 2016, Shindy et al, 2015, Shindy et al., 2015a, Shindy, 2012, Shindy et al., 2014) essentially arises from their applications and uses in various research field (Shershof, et al., 2013, Leevy, et al., 2008, Zhang, et al., 2004 and Savitsky, et al. 2004, Li et al., 2006, Wang, et al., 2007, Licha, et al., 2000). Such as biochemistry, molecular biology, bio-medicine and structural biology. In addition, cyanine dyes are frequently used as reporter groups for labeling proteins, DNA sequencing, oligoonucleotides and antibodies (Wang et al., 2009, Zhang et al., 2008, Peng et al., 2008, Pham et al., 2005, Chen et al., 2005, Zheng et al., 2002). Besides, these dyes attract much attention because of their application in a number of research area such as probes for the determination of solvent polarity, potential applications for colorimetric sensor (Bamfield, 2001, Janzen et al., 2006), as photographic sensitizers and in chemotherapy (Toutchkine et al., 2007, Wröblewska et al., 2005, Rösch et al., 2006, Würthner et al., 2006, Martins et al., 2006, Leng et al., 2005).

Taking in consideration the above benefits of cyanine dyes we prepared here new polyhetrocyclic moonomethine and trimethine cyanine dyes as new synthesis contribution, spectral sensitization, solvatochromic and halochromic evaluation to may be used and/or applied in any of the wide range applications of cyanine dyes, particularly as photographic sensitizers for silver

* Corresponding author
E-mail addresses: hashindy2@hotmail.com (H A. Shindy)

halide emulsion in photographic industry, as probes to determining solvent polarity in solution chemistry and/or as pH indicators in operations of acid/base titrations in analytical chemistry.

2. Results and discussion

2.1-Synthesis:

Reaction of 3-methyl-1-phenyl-5-pyrazolone (1) with 4-bromo-3-methyl-1-phenyl-5-pyrazolone (2) in equimolar ratios in ethanol containing pyridine achieved 4,5-dimethyl-2,7-diphenyl-furo[(3,2-d), ($\bar{3},\bar{2}$-d)] bis pyrazole (3) as new heterocyclic starting material compound, Scheme (1).

Quaternization of (3) using excess of iodoethane resulted its 3,6-di iodoethane quaternary salt compound (4), Scheme (1).

Reaction of the quaternary salt (4) with 1-ethylpyridinum-4-yl salt, 1-ethyl quinolinum-4- yl salt and/or 2-ethyl isoquinolinum-1-yl salt in 1:2 molar ratios and in ethanol as organic solvent containing few mls of piperidine gives the 4,5-[4(1)]-bis monomethine cyanine dyes (5a-c), Scheme (1).

1:2 molar ratios of the quaternary salts (4) and triethylorthoformate (triethoxy methane) were reacted in ethanol containing piperidine and produced the intermediate compound (6). Further reaction of the intermediate compound (6) in 1:2 molar ratios with 1-ethyl pyridinium-2-yl salt, 1-ethyl quinolinium-2-yl salt and/or 1-ethyl pyridinium-4-yl salt in ethanol and in presence of piperidine achieved the 4,5-[2(4)]-bis trimethine cyanine dyes (7a-c), Scheme (1).

The structure of the prepared compounds were identified by elemental analysis (Tables 1, 2), visible spectra (Tables 1, 2), mass spectrometer, IR (Wade, 1999) and ^{1}H NMR (Wade, 1999a) spectral data (Table 3).

2.2-Spectral sensitization evaluation:

Spectral sensitization evaluation for all the synthesized cyanine dyes was carried out through investigating their electronic visible absorption spectra in 95 % ethanol solution. The dyes are thought to be better spectral sensitizers when they absorb light at longer wavelength bands (bathochromic shifted and/or red shifted dyes). Consequently the spectral sensitization of the dyes decrease when they absorb light at shorter wavelength bands (hypsochromic shifted and/or blue shifted dyes). So, we may say that the spectral sensitization of one dye is higher than the other one if the wavelength of the maximum absorption spectrum of the former is longer than that of the latter. Inversely, we may say that the spectral sensitization of one dye is lower than the other one if the wavelength of the maximum absorption spectrum of the former is shorter than that of the latter.

The electronic visible absorption spectra of the monomethine cyanine dyes (5a-c) in 95 % ethanol solution discloses bands in the visible region (380-440 nm). The positions of these bands and their molar extinction coefficient (molar absorptivity) are largely effected by the types of heterocyclic quaternary salts residue (A) and their linkage positions. So, substituting, A = 1-ethyl-pyridinium-4-yl salt by A = 1-ethyl-quinolinium-4-yl salt moving from dye (5a) to dye (5b) caused bathochromic shifts for the absorption bands by (20 nm), Scheme (1), Table (1). This can be attributed to increasing π-delocalization in the latter dye (5b) due to the presence of quinoline ring system in correspondence to pyridine ring system in the former dye (5a). Changing the linkage position from 1-ethyl-quinolinium-4-yl salt to 2-ethyl isoquinolinium-1-yl salt, transferring from dye (5b) to dye (5c) resulted a hypsochromic shifts for the absorption bands by (12 nm), Scheme (1), Table (1). This can be related to decreasing the length of the π-delocalization conjugation in latter dye (5c) due to the presence of isoquinoline ring system in correspondence to quinoline ring system in the former dye (5b).

Additionally, the electronic visible absorption spectra of the trimethine cyanine dyes (7a-c) in 95 % ethanol solution reveals bands in the visible range (438-620 nm). The positions of these bands underwent displacements to give bathochromic shifts (red shifts) and/or hypsochromic shifts (blue shifts) in addition to increasing and/or decreasing the number and the intensity of the absorption bands depending upon the type of the heterocyclic quaternary salt residue (A) and their linkage positions, Scheme (1), Table (2). So, substituting pyridinium salt residue in dye (7a) by quinolinium salt residue to get dye (7b) caused strong bathochromic shifts for the absorption bands by (140 nm) in addition to increasing the number of the absorption bands, Scheme (1), Table (2). This can be attributed to increasing conjugation in the latter dye (7b) due to the presence

quinaldine nucleus in corresponding to α-picoline nucleus in the former dye (7a). Changing the linkage position from 2-yl salt residue in dye (7a) to 4-yl salt residue to obtain dye (7c) resulted bathochromic shifts (red shifts) for the bands by (60 nm) accompanied by increasing the number of the bands, Scheme (1), Table (2). This can be related to increasing the length of the conjugation in the latter dye (7c) due to the presence of γ-picoline nucleus in correspondence to α-picoline nucleus in the former dye (7a).

General comparison for the electronic visible absorption sopectra of the monomethine cyanine dyes (5a-c) with those of the trimethine cyanine dyes (7a-c) displayed that the latter dyes have bathochromically shifted bands than the former dyes, Tables (1, 2). This can be explained in the light of increasing the number of methine groups in the latter dyes, Scheme (1).

2.3-Solvatochromic evaluation:

Solvatochromic evaluation for some selected synthesized cyanine dyes (5b) and (7b) was carried out via examining of their electronic visible absorption spectra in pure solvents having different polarities. The dyes are though to be better solvatochromic dyes when they give a remarkable positive solvatochromism and/or negative solvatochromism in these solvents. Positive solvatochromism reveals bathochromic shifted (red shifted) absorption bands with increasing solvent polarity. Inversely, negative solvatochromism discloses hypsochromic shifted (blue shifted) bands with increasing solvent polarity. This study was carried out to select the best solvents to use of these dyes as photosensitizers when they are used and/or applied in photosensitive material industry. The other important purpose of these study is to evaluate the solvatochromic properties of these dyes to may be use and/or applied as probes for determining solvent polarity in physical, physical organic and/or inorganic chemistry.

So, the electronic visible absorption of the monomethine cyanine dye (5b) and the trimethine cyanine dyes (7b) in pure solvents of different polarities (different dielectric constant) namely water (78.54), DMF (36.70), ethanol (24.3), chloroform (4.806), carbontetrachloride (2.238) and dioxane (2.209) (Shindy, et al, 2015b, Shindy, et al, 2016a) are recorded. The λ_{max} (wavelength) and ε_{max} (molar extinction coefficients) values of the absorption bands due different electronic transitions within the solute molecule in these solvents are represented in Table (4).

From Table (4) its clearly that the electronic visible absorption spectrum of the dyes (5b) and (7b) in ethanolic medium are characterized by the presence of two (dye 5b) and/or three (dye7b) essential absorption bands. These bands can be assigned to intermolecular charge transfer transition (Shindy, et al., 2015b, Shindy, et al., 2016a). These charge transfer is due to transfer of lone pair of electrons from the N-ethyl pyrazole nitrogen atom to the positively charged quaternary nitrogen atom of the quinolinium salt residue, Scheme (2).

The data given in Table (4) show that the charge transfer band exhibits a hypsochromic shift in ethanol relative to DMF, dioxane, chloroform and carbontetrachloride. These effects may be attributed to the following factors:

a-The bathochromic shift in DMF relative to ethanol is a result of the increase in solvent polarity due to the increasing of dielectric constant of DMF relative to ethanol.

b-The hypsochromic shift occurs in ethanol relative to dioxane, chloroform and carbontetrachloride is a result of the solute solvent interaction through intermolecular hydrogen band formation between ethanol and the lone pair electrons of the N-ethyl pyrazole nitrogen atom, Scheme (3) (A). This decreases slightly the electron density on the N-ethyl pyrazole nitrogen atom and consequently decreases to some extent the mobility of the attached π-electrons over the conjugated system pathway to the positively charged quaternary nitrogen atom of the quinolinium salt residue, and consequently a hypsochromic shift occurs.

Also, from the data given in Table (4) it is observed that occurrence of unexpected hypsochromic shifts in water relative to ethanol and the other solvents. This can be mainly ascribed to the possible interaction of water molecules with the lone pair electrons of the N-ethyl pyrazole nitrogen atom, Scheme (3) (B). This makes difficult the transfer of electronic charge from the N-ethyl pyrazole nitrogen atom to the quaternary nitrogen atom of the heterocyclic quinolinium salt residue, and accordingly there is observed a hypsochromic shift in water relative to ethanol and the other solvents.

2.4-Halochromic evaluation:

Halochromic evaluation for some selected synthesized cyanine dyes (5b) and (7b) was carried out by investigating of their electronic visible absorption spectra in aqueous universal buffer solutions having varied pH values, Table (5). The dyes are though to be better halochromic dyes when they give a noticeable positive halochromism and/or negative halochromism in these buffer solutions. Positive halochromism means occurrence of a bathochromic shifted (red shifted) absorption bands with changing solution pH of the buffer solution. In contrast negative halochromism means occurrence of a hypsochromic shifted (blue shifted) absorption bands with changing the pH of the buffer solution.

The solutions of the bis monomethine cyanine dyes (5b) and the bis trimethine cyanine dyes (7b) have a permanent cationic charge in basic media that then discharged on acidification. This prompted and encouraged us to study their spectral behaviour in different buffer solutions in order to select a suitable pH for use of these dyes as photosensitizers. The other purpose of this study is to evaluate the halochromic properties of these dyes to may be used and/or applied as pH indicators in acid / base titration in analytical chemistry. The acid dissociation or protonation constant of these dyes have been determined. The effect of the compounds as photosensitizers increases when they are present in the ionic form, which has a higher planarity (Shindy, et al., 2015b, Shindy, et al., 2016a) and therefore more conjugation.

So, the electronic visible absorption spectra of the bis monomethine cyanine dye (5b) and the bis trimethine cyanine dye (7b) in aqueous universal buffer solutions of varying pH values (1.75, 2.45, 4.65, 5.80, 7.88, 8.75, 10.85 and 12.60 units) showed bathochromic shifted bands at high pH media (alkaline media) and hypsochromic shifted bands at low pH media (acidic media). So, the mentioned dyes which has lone pair of electrons on the N-ethyl pyrazole nitrogen atom undergoes to protonation in low pH media (acidic media). This leads to a criterion of positive charge on the N-ethyl pyrazole nitrogen atom and consequently the electronic charge transfer pathways to the quaternary heterocyclic quinolinium salt residue will be difficult resulting in a hypsochromic shift for the absorption bands (protonated and/or colourless-yellow structure), Scheme (4) (A).

On increasing the pH of the media, the absorption bands are bathochromically shifted due to the deprotonation of the N-ethyl pyrazole nitrogen atom, and consequently the electronic charge transfer pathways to the quaternary heterocyclic quinolinium salt residue will be easier and facilitated resulting in a bathochromic shift for the absorption bands (deprootonated and/or coloured structure), Scheme (4) (B).

Several methods have been developed for the spectrophotometric determination of the dissociation constants of weak acids. The variation of absorbance with pH can be utilized. On plotting the absorbance at fixed λ vs. pH, S-shaped curves are obtained, Table (6). An all of the S-shaped curves obtained the horizontal portion to the left corresponds to the acidic form of the indicator, while the upper portion to the right corresponds to the basic form of the indicator, since the pka is defined as the pH value for which one half of the indicator is in the basic form and the other half is in the acidic form. This point is determined by intersection of the curve with a horizontal line midway between the left and right segments (Shindy, et al., 2015b, Shindy, et al., 2016a). The acid dissociation or protonation constants values of the dyes (5b) and (7b) are given in Table (6).

3. Conclusion

Following are major conclusions were extracted from the results discussed in this investigation:

1-The electronic visible absorption spectra of the 4,5-[4(1)]-bis monomethine (5a-c) and the 4,5-[2(4)]-bis trimethine (7a-c) cyanine dyes in 95 % ethanol underwent displacements to give bathochromic and/or hypsochromic shifts accompanied by increasing and/or decreasing the number and the intensity of the bands depending upon the following factors:

a-Types of the heterocyclic quaternary salt residue in the order of:

(I) quinolinium dyes > pyridinium dyes (for the bis monomethine cyanine dyes).

(II) quinaldinum dyes > α-picolinium dyes (for the bis trimethine cyanine dyes).

b-Linkage positions of the heterocyclic quaternary salts in the order of:

(I)quinolinium dyes > isoquinolinium dyes (for the bis monomethine cyanine dyes.

(II) γ-picolinium dyes > α-picolinium dyes (for the bis trimethine cyanine dyes.

c-Increasing number of the methine units in the order of:

Trimethine cyanine dyes > monomethine cyanine dyes.

2-The intensity of the colours of the bis monomethine cyanine dyes (5a-c) and the bis trimethine cyanine dyes (7a-c) can be illustrated in the light of the two suggested mesomeric structures (A) and (B) producing a delocalized positive charge over the conjugated system, Scheme (2).

3-The solvatochromism of the examined cyanine dyes (5b) and (7b) in pure solvents having different polarities underwent displacements to give positive solvatochromism (occurrence of a bathochromic shift with increasing solvent polarity) and/or negative solvatochromism (occurrence of a hypsochromic shift with increasing solvent polarity) depending upon the following factors:

a-Increasing and/or decreasing the polarity (dielectric constant) of the solvents (General solvent effect).

b-Hydrogen bond and/or molecular complex formation between the solute (dyes molecules) and the solvent used (specific solvent effect).

4-The halochromism of the monomethine cyanine dye (5b) and the bis trimethine cyanine dye (7b) in aqueous universal buffer solutions having varying pH values underwent to give the following displacements changes in their absorption spectra wavelength bands:

a-Hypsochromic shifted bands in the lower pH media (acidic media) due to the protonated and/or colourless structures of the dyes in this media. b-Bathochromic shifted bands in the higher pH media (basic media) due to the deprotonated and/or coloured structures of these dyes in this media.

5-These cyanine dyes can be used as:

a-Photographic sensitizers for silver halide emulsion in photographic industry due to their spectral and/or photosensitization properties.

b-Indicators for solvent polarity in solution chemistry due to their solvatochromic properties.

c-Acid-base indicators in analytical chemistry due to their halochromic properties

4-Experimental

4.1-General:

All the melting points of the prepared compounds are measured using Electrothermal 15V, 45W 1 A9100 melting point apparatus, Chemistry department, Faculty of Science (Aswan University) and are uncorrected. Elemental analysis were carried out at the Microanalytical Center of Cairo University by an automatic analyzer (Vario EL III Germany). Infrared spectra were measured with a FT/IR (4100 Jasco Japan), Cairo University. ^{1}H NMR Spectra were accomplished using Varian Gemini-300 MHz NMR Spectrometer (Cairo University). Mass Spectroscopy was recorded on Mas 1: GC-2010 Shimadzu Spectrometer (Cairo University). Electronic visible absorption spectra were carried out on Visible Spectrophotometer, Spectro 24 RS Labomed, INC, Chemistry department, Faculty of Science (Aswan University).

4.2-Synthesis:

4.2.1-Synthesis of 4,5-dimethyl-2,7-diphenyl-furo [(3,2-d), (3,2-d) bis pyrazole] (3).

A mixture of equimolar ratios (0.01 mol) of 3-methyl-1-phenyl-5-pyrazolone (l) and 4-bromo-3-methyl-1-phenyl-5- Pyrazolone (2) was dissolved in ethanol (30 ml) containing pyridine (5-10 ml). The reaction mixture was heated under reflux for 6-8hrs, and changed its colour from reddish to deep brown at the end of refluxing. It was filtered while hot to remove any impurities and precipitated by ice-water mixture. The product were collected, dried and crystallized from ethanol. The results are listed in Table (1).

4.2.2-Synthesis of 3, 6-diethyl 4, 5-dimetyl -2, 7-diphenyl-furo [(3, 2-d), (3 2-d) bis pyrazolium] diiodie salts (4).

A pure crystallized sample of (3) (0.01 mol) and excess of bimolar ratios of iodoethane were heated in a sealed tube till complete fusion. The products were cooled, dissolved in ethanol (30 ml), and heated under reflux for 1 hour. The reaction mixtures were filtered while hot to remove impurities, concentrated and cooled. The precipitates were collected, dried, and crystallized using ethanol, see the data in Table (1).

4.2.3-Synthesis of 3,6-diethyl-2,7-diphenyl-furo[(3, 2-d), ($\bar{3},\bar{2}$-d) bis pyrazole]-4,5[4(1)]-bis monomethine cyanine dyes (5a-c).

A mixture of (4) (0.01 mol) and bimolar ratios of N-ethyl (pyridinum, quinolinum or isoquinolinuim) salts were dissolved in ethanol (30 ml) containing piperidine (1-2 mls). The reaction mixtures were heated under reflux for 6 hrs. It was filtered off while hot to remove any impurities, cooled, and precipitated by dilution with ice-water mixture with continues shaking. The precipitates were filtered, washed with water several times, dried and crystallized from ethanol. The relevant data are given in Table (1).

4.2.4-Synthesis of 3,6-diethyl-2,7-diphenyl-furo [(3, 2-d), ($\bar{3},\bar{2}$-d) bis pyrazolium]-4,5[1,1-diethoxy ethyl] diiodide salt as intermediate compound (6).

1:2 molar ratios of the quaternary salt compound (4) and triethylorthoformate were heated under reflux in ethanol (30 ml) containing piperidine (1-2 mls) for 6 hrs, until it gave a permanent deep colour at the end of refluxing. The reaction mixture was filtered off while hot to remove impurities, concentrated to one half of its volume, cooled, and precipitated by cold water. The precipitates were filtered, washed with water several times, dried and crystallized from ethanol. The data were recorded in Table (2).

4.2.5-Synthesis of 3,6- diethyl 2,7-diphenyl-furo[(3, 2-d), ($\bar{3},\bar{2}$-d)) bis pyrazole] - 4, 5 [2 (4)] -bis trimethine cyanine dyes (7a - c).

A mixture of unimolar ratio (0.01 mol) of the intermediate compound (6) and bimolar ratio (0.02 mol) of N-ethyl (2-picolinium, quinaldinium, or 4-picolinuim) iodide quaternary salts were dissolved in ethanol (30 ml) containing piperidine (1-2 mls). The reaction mixture was heated under reflux for 6 hrs, and attained highly violet colours at the end of ref1uxing. The mixture was filtered off while hot, precipitated by dilution with ice-water mixture with continues shaking. The precipitates were filtered off, washed with water several times dried and crystallized from ethanol. The data were registered in Table (2).

4.3-Visible absorption spectra:

The electronic visible absorption spectra of the prepared cyanine dyes were examined in 95 % ethanol solution and recorded using 1cm Qz cell in Vis Spectrophotometer, Spectro 24RS Labomed, INC. A stock solution (1 x 10^{-3}M) of the dyes was prepared and diluted to a suitable volume in order to obtain the desired lower concentrations. The spectra were recorded immediately to eliminate as much as possible the effect of time.

4.4-Solvatochromism and halochromis:

The electronic visible absorption spectra of some selected synthesized cyanine dyes were investigated in pure organic solvents of spectroscopic grade (Shindy, et al., 2015b, Shindy, et al., 2016a) and different polarities and/or in aqueous universal buffer solutions having varying pH values and recorded using 1cm quartz cell in Vis Spectrophotometer Spectro 24 RS Labomed, INC. A stock solution (1 x 10^{-3}M) of the dyes was prepared and diluted to a suitable volume using the suitable solvent and/or the buffer solution to obtain the required lower concentrations. The spectra were recorded immediately to eliminate as much as possible the effect of time.

5. Acknowledgements

We are thankful to the Chemistry department, Faculty of Science, Aswan University, Aswan, Egypt for supporting this work.

References

Shindy et al., 2012 – *Shindy, H. A., El-Maghraby, M. A., Eissa, F. M.* (2012). Synthesis and Colour Spectrophotometric Measurements of some Novel Merocyanine dyes. *Dyes and Pigments*, 92 (3), 929-935.

Shindy et al., 2016 – *Shindy, H. A., Khalafalla, A. K., Goma, M. M., Eed, A. H.* (2016). Polylyheterocyclic compound in the synthesis and spectral studies of some novel methine cyanine dyes. *Revue Roumaine de Chimie*, 61 (3), 139-145.

Shindy et al., 2015 – *Shindy, H. A., Goma, M. M., Harb, N. A.* (2015). Synthesis, Spectral Behavior and Biological Activity of some Novel 1,3,4-Oxadiazine Cyanine Dyes. *European Journal of Chemistry*, 6 (2), 151-156.

Shindy et al., 2015a – *Shindy, H. A., Khalafalla, A. K., Goma, M. M., Eed, A. H.* (2015). Synthesis and photosensitization evaluation of some novel polyheterocyclic cyanine dyes. *European Reviews of Chemical Research*, 5 (3), 180-188.

Shindy, 2012 – *Shindy, H. A.* (2012). Synthesis of different classes of five/five membered heterocyclic cyanine dyes: *A Review paper, Mini-Reviews in Organic Chemistry*, 9 (2), 209-222.

Shindy et al., 2014 – *Shindy, H. A., El-Maghraby, M. A., Eissa, F. M.* (2014). Effects of Chemical structure, solvent and solution pH on the visible spectra of some new methine cyanine dyes. *European Journal of Chemistry*, 5 (3), 451-456.

Shershof et al., 2013 – *Shershof V. E., Spitsyn, M. A., Kuznetsova, V. E., Timofeev, E. N., Ivashkina O. A., Abranov, I. S., Nasedkina, T. V., Zasedatelev, A. S.* (2013). Near infrared heptamethine cyanine dyes. Synthesis, spectroscopic characterization, thermal properties and photostability, *Dyes and pigments*, 97, 353-360.

Leevy et al., 2008 – *Leevy, W. M., Gammon, S. T., Johnson, J. R., Lampkins, A. J., Jiang, H., Marquez, M., et al.* (2008). Noninvasive optical imaging of Staphylococcus aureus bacterial infection in living mice using a bis-dipicolylamine-zinc(II) affinity group conjugated to a near-infrared fluorophore. *Bioconjug Chem*, 19 (3), 686-92.

Zhang et al., 2004 – *Zhang, Z., Bloch, S., Achilefu, S.* Synthesis and evaluation of novel galactose-carbocyanine fluorescent contrast agents with enhanced hydrophilicity and rigid molecular constraint. Photonics West 2004, Biomedical Optics (BiOS), Sept. 3, Bellingham, W. A., USA. In: Savitsky, et al. 2004. Savitsky, A. P. Bornhop D. J., Raghavachari, R, Achilefu S. I. , editors. Genetically engineered and optical probes for biomedical applications II. p. 262-8.

Li et al., 2006 – Li, C., Greenwood, T. R., Bhujwalla, Z. M., Glunde, K. (2006). Synthesis and characterization of glucosamine-bound near-infrared probes for optical imaging. Org Lett, 8 (17), 3623-6.

Wang et al., 2007 – *Wang, W., Ke, S., Kwon, S., Yallampalli, S., Cameron, A. G., Adams, K. E. et al.* (2007). A new optical and nuclear dual-labeled imaging agent targeting interleukin 11 receptor alpha-chain. Bioconjug Chem, 18 (2), 397-402.

Licha et al., 2000 – *Licha, K., Riefkea, B., Ntziachristosb, V., Beckerd, A., Chancee, B., Semmlerf, W.* (2000). Hydrophilic cyanine dyes as contrast agents for near-infrared tumor imaging: synthesis, photophysical properties and spectroscopic in vivo characterization. Photochem Photobiol 2000, 72 (3), 392-8.

Wang et al., 2009 – *Wang, S., Kim, S.* (2009). New solvatochromic merocyanine dyes based on barbituric acid and Meldrum's acid, Dyes and pigments, 80 (3), 314-320.

Zhang et al., 2008 – *Zhang, S., Metelev, V., Tabatadze, D., Zamecnik, P. C., Bogdanov, A.* (2008). Fluorescence resonance energy transfer in near-infrared fluorescent oligonucleotide probes for detecting protein-DNA interactions. Proc Natl Acad Sci USA, 105 (11), 4156-61.

Peng et al., 2008 – *Peng, X., Chen, H., Draney, D. R., Volcheck, W., Schutz-Geschwender, A., Olive, D. M.* (2008). A non-fluorescent, broad range quencher dye for FRET assays, Anal Biochem, 388 (2), 220-8.

Pham et al., 2005 – *W., Medarova, Z., Moore, A.* (2005). Synthesis and application of a water-soluble near-infrared dye for cancer detection using optical imaging. Bioconjug Chem, 16 (3), 735-40.

Chen et al., 2005 – *Chen, Y., Grushuk, A., Achilefu, S., Ohylchansky, T., Potter, W., Zhong, T., et al.* (2005). A novel approach to a bifunctional photosensitizer for tumor imaging and photo-therapy. Bioconjug Chem, 16 (5), 1264-74.

Zheng et al., 2002 – *Zheng, G., Li, H., Yang, K., Blessington, D., Licha, K., Lund-Katz S. et al.* (2002). Tricarbocyanine cholesteryl labeled LDL: new near infrared fluorescent probes (NIRFs) for monitoring tumors and gene therapy of familial hypercholesterolemia, Bioorg Med Chem Lett., 12 (11), 1485-8.

Bamfield, 2001 – *Bamfield, P.* (2001). Chromic phenomena: technological application of colour chemistry. The Royal Society of Chemistry, Cambridge. UK.

Janzen et al., 2006 – Janzen, M. C., Ponder, J. R., Bailey, D. P., lngison, C. K., Suslick, K. S. (2006). Colorimetric sensor arrays for volatile organic compounds. *Analytical chemistry*, 78 (11), 3591-6000.

Toutchkine et al., 2007 – *Toutchkine, A., Nguyen, D. V., Hahn, K. M.* (2007). Merocyanine dyes with improved photostability. Organic Letter, 9 (15), 2775-7.

Wröblewska et al., 2005 – *Wröblewska, E. K., Soroka, J. A., Soroka, K. B., Gasiorowska, M.* S. (2005). solvatochromism of dyes. Part IV – energetic characteristics of merocyanine derivatives of 1-phenyl-2-[2-(3-X-4-hydroxy-5-R -phenyl)-3-3-dimethyl-3H-indolium cation. *Journal of Physical Organic Chemistry*, 18, 347-52.

Rösch et al., 2006 – *Rösch, U., Yao, S., Wortmann, R., Würthner, F.* (2006). Fluorescent H-aggregates of merocyanine dyes. *Angewandte Chemie International. Edition*, 45, 7026-30.

Würthner et al., 2006 – *Würthner, F., Schmidt, J., Stolte, M., Wortmann, R.* (2006). Hydrogen-band-directed head-to-tail orientation of dipolar merocyanine dyes: a strategy for the design of electrooptical materials. Angewandte Chemie international Edition, 45, 3842-6.

Martins et al., 2006 – *Martins, C. T., Lima, M. S., El-Seoud, O. A.* (2006). Thermosolvatochromism of merocyanine polarity indicators in pure and aqueous solvents: relevance of solvent lipophilicity. *Journal of Organic Chemistry*, 71 (24), 9068-79.

Leng et al., 2005 – *Leng, W., Wurthner, F., Kelley, A. M.* (2005). Solvent-dependent vibrational frequencies and reorganization energies of two merocyanine chromophores. *The journal of Physical Chemistry A*, 109 (8), 1570-5.

Wade, 1999 – *Wade, Jr., L. G.* Organic. Chemistry., 4th Edn., Pearson Educ., (Prentice Hall, Upper Saddle River, New Jersy 07458, USA), 1999, 500-538.

Wade, 1999a – Wade, Jr., L. G., Organic. Chemistry., 4th Edn., Pearson Educ. (Prentice Hall, Upper Saddle River, New Jersy 07458, USA), 1999, 544-604.

Shindy et al., 2015b – *Shindy, H. A., Goma, M. M.,Harb, N. A.* (2015). Synthesis, Structure/Spectra Correlation and Chromism Studies of some Novel Monomethine and Bis-Monomethine Cyanine Dyes. *European Reviews of Chemical Research*, 4 (2), 126-140.

Shindy et al., 2016a – Shindy, H. A., Goma, M. M., Harb, N. A. Novel carbocyanine and bis carbocyanine dyes: synthesis, visible spectra studies, solvatochromism and halochromism. *Chemistry International*, 2 (4), 222-231.

Appendix

Table 1. Characterization of the prepared compounds (3), (4) and (5a-c)

Comp. No	Nature of product			Molecular formula (M.Wt.)	Analysis %						Absorption spectra in 95% ethanol solution	
					Calculated			Found				
	Colour	Yield (%)	M.P. (°C)		C	H	N	C	H	N	λ_{max} (nm)	ε_{max} (mole-1cm²)
3	Brown	65	190	$C_{20}H_{16}N_4O$ (328)	73.17	4.87	17.07	73.15	4.85	17.04	----	------
4	Deep brown	55	175	$C_{24}H_{26}N_4OI_2$ (640)	45.00	4.06	8.75	44.98	4.04	8.73	-----	------
5a	Red	45	160	$C_{38}H_{40}N_6OI_2$ (850)	53.64	4.70	9.88	53.62	4.68	9.86	380, 420	2286, 2278
5b	Deep red	59	140	$C_{46}H_{44}N_6OI_2$ (950)	58.10	4.36	8.84	58.00	4.34	8.82	400, 440	2286, 2242
5c	Deep red	53	155	$C_{46}H_{44}N_6OI_2$ (950)	58.10	4.36	8.84	58.00	4.34	8.82	395, 428	2267, 2246

Table 2. Characterization of the prepared compounds (6) and (7a-c)

Comp. No	Nature of product			Molecular formula (M.Wt.)	Analysis %						Absorption spectra in 95% ethanol solution	
	Colour	Yield (%)	M.P. (°C)		Calculated			Found			λ_{max} (nm)	ε_{max} (mole-1cm²)
					C	H	N	C	H	N		
6	Brown	62	150	$C_{34}H_{46}N_4O_5I_2$ (844)	48.34	5.45	6.63	48.32	5.44	6.60	---	---
7a	Violet	51	120	$C_{40}H_{44}N_6OI_2$ (878)	54.66	5.01	9.56	54.63	5.00	9.54	438, 480	2276, 2225
7b	Deep violet	65	145	$C_{50}H_{48}N_6OI_2$ (1002)	59.88	4.79	8.38	59.86	4.75	8.36	460, 560, 620	2275, 2244, 2220
7c	Deep violet	48	100	$C_{40}H_{44}N_6OI_2$ (878)	54.66	5.01	9.56	54.63	5.00	9.54	440, 480, 540	2276, 2251, 2223

Table 3. IR and ^{1}H NMR (mass) spectral data of the prepared compounds (3), (4), (5b), (6) and (7b)

Comp. No	IR Spectrum (KBr, Cm^{-1})	^{1}H NMR Spectrum (DMSO, δ); & (Mass data)
3	687, 754(monosubstituted phenyl). 1031, 1073, 1111, 1172(C-O-C cyclic). 1328, 1367 (C-N). 1495, 1457 (C=N). 1617, 1594 (C=C).	2.2 (m, 6H, $2CH_3$ of positions 4 and 5). 7.2-8 (m, 10H, aromatic). M^++1: 328.89
4	690, 756 (monosubstituted phenyl). 1034, 1072, 1119, 117 (C-O-C cyclic). 1362 (C-N) 1457, 1497 (C=N). 1597, 1551 (C=C). 2922 (quaternary salt).	2.2 (m, 6H, $2CH_3$ of positions 4, 5). 2.3-2.4 (m, 6H, $2CH_3$ of positions 3, 6). 3.5 (m, 4H, $2CH_2$ of positions 3, 6). 7.2-8 (m, 10H, aromatic). M^+: 640
5b	692, 757 (monosubstituted phenyl). 809, 833, 875 (o.disubstituted phenyl). 1025, 1119, 1164 (C-O-C cyclic). 1351 (C-N) 1489, 1525 (C=N). 1596 (C=C). 2924, 2855 (quaternary salt).	2.25 (m, 6H, $2CH_3$ of positions 3, 6). 3.00 (s, 4H, $2CH_2$ of positions 3, 6). 1.5 (m, 6H, $2CH_3$ of quinolinium). 3.3 (s, 4H, $2CH_2$ of quinolinium). 7-8.5 (m, 24H, aromatic + heterocyclic + 2-CH=).
6	756, 691 (monosubstituted phenyl). 1027, 1066, 1126, 1193 (C-O-C cyclic). 1358 (C-N). 1496, 1447 (C=N). 1596, 1553 (C=C). 2924, 2854 (quaternary salt).	1.35 (m, 12H, $4CH_3$ of diethoxyethyl). 2.3-2.4 (m, 6H, $2CH_3$ of positions 3, 6). 3.6 (m, 4H, $2CH_2$ of positions 3, 6). 3.7 (m, 8H, $4CH_2$ of diethoxyethyl). 3.8 (m, 4H, $2CH_2$ of positions 4. 5). 4.2 (m, 2H, 2CH of positions 4. 5). 7-8.2 (m, 10H, aromatic). M^+: 844.12
7b	600, 755 (monosubstituted phenyl). 876 (o.disubstituted phenyl). 1032, 1121, 1158 (C-O-C cyclic). 1437 (C=N). 1629 (C=C). 2926 (quaternary salt).	1.2-1.5 (m, 6H, $2CH_3$ of positions 3, 6). 2.1-2.3 (m, 4H, $2CH_2$ of positions 3, 6). 2.9-3 (m, 6H, $2CH_3$ of quinolinium). 3.2-3.8 (b, 4H, $2CH_2$ of quinolinium). 7-8.5 (m, 28H, aromatic + heterocyclic + 6-CH=).

Table 4. Solvatochromism of the dyes (5b) and (7b) in pure solvents having different polarities

Solvent / Dye No.	H_2O		EtOH		DMF		$CHCl_3$		CCl_4		Dioxane	
	λ_{max} (nm)	ε_{max} ($mol^{-1}cm^2$)	λ_{max} (nm)	ε_{max} ($mol^{-1}cm^2$)	λ_{max} (nm)	ε_{max} ($mol^{-1}cm^2$)	λ_{max} (nm)	ε_{max} ($mol^{-1}cm^2$)	λ_{max} (nm)	ε_{max} ($mol^{-1}cm^2$)	λ_{max} (nm)	ε_{max} ($mol^{-1}cm^2$)
5b	410 430	1342 1318	400 440	2286 2242	430 450 520	1366 1398 1729	420 450	1649 1184	420 450 480	1764 1784 1813	420 450 490	1270 1288 1281
7b	430 460 555	1186 1309 877	460 560 620	2275 2244 2220	430 450 550 640	1583 1550 1893 642	430 470 625	1094 1175 594	420 460 480 550 630	1544 1550 1721 1820 687	450 480 580 635	1140 1154 828 374

Table 5. Halochromism of the dyes (5b) and (7b) in aqueous universal buffer solutions having varying pH values

pH / Dye No.	Universal Buffers															
	1.75		2.45		4.65		5.8		7.88		8.75		10.58		12.6	
	λ_{max} (nm)	ε_{max} ($mol^{-1}cm^2$)	λ_{max} (nm)	ε_{max} ($mol^{-1}cm^2$)	λ_{max} (nm)	ε_{max} ($mol^{-1}cm^2$)	λ_{max} (nm)	ε_{max} ($mol^{-1}cm^2$)	λ_{max} (nm)	ε_{max} ($mol^{-1}cm^2$)	λ_{max} (nm)	ε_{max} ($mol^{-1}cm^2$)	λ_{max} (nm)	ε_{max} ($mol^{-1}cm^2$)	λ_{max} (nm)	ε_{max} ($mol^{-1}cm^2$)
5b	400 420 540	2327 1971 713	420 435 555	1707 1567 1425	425 450 560	1764 1910 595	435 460 562	1644 1473 922	440 462 565	2289 2234 1036	445 468 570	1248 1196 802	445 470 572	2372 1857 877	445 474 575	2471 2151 946
7b	440 480 590	2007 1452 796	450 480 592	1098 1143 634	450 482 594	1467 1355 745	450 482 595	2266 1804 865	450 485 597	1815 1567 679	450 490 598	1176 1023 711	452 495 600	1069 1087 675	455 498 610	1052 1043 653

Table 6. The variation of absorbance with pH at fixed λ for the dyes (5b) and (7b) in aqueous universal buffer solutions

		pH								
	Dye	**1.75**	**2.45**	**4.65**	**5.8**	**7.88**	**8.75**	**10.58**	**12.6**	**PKa**
Absorbance at fixed wavelength	**5b** **λ=510(nm)**	0.978	0.669	0.866	0.898	0.813	0.801	1.144	1.354	4.5 8.7
	7b **λ=590(nm)**	0.796	0.634	0.745	0.865	0.679	0.711	0.466	0.49	4.6 10.2

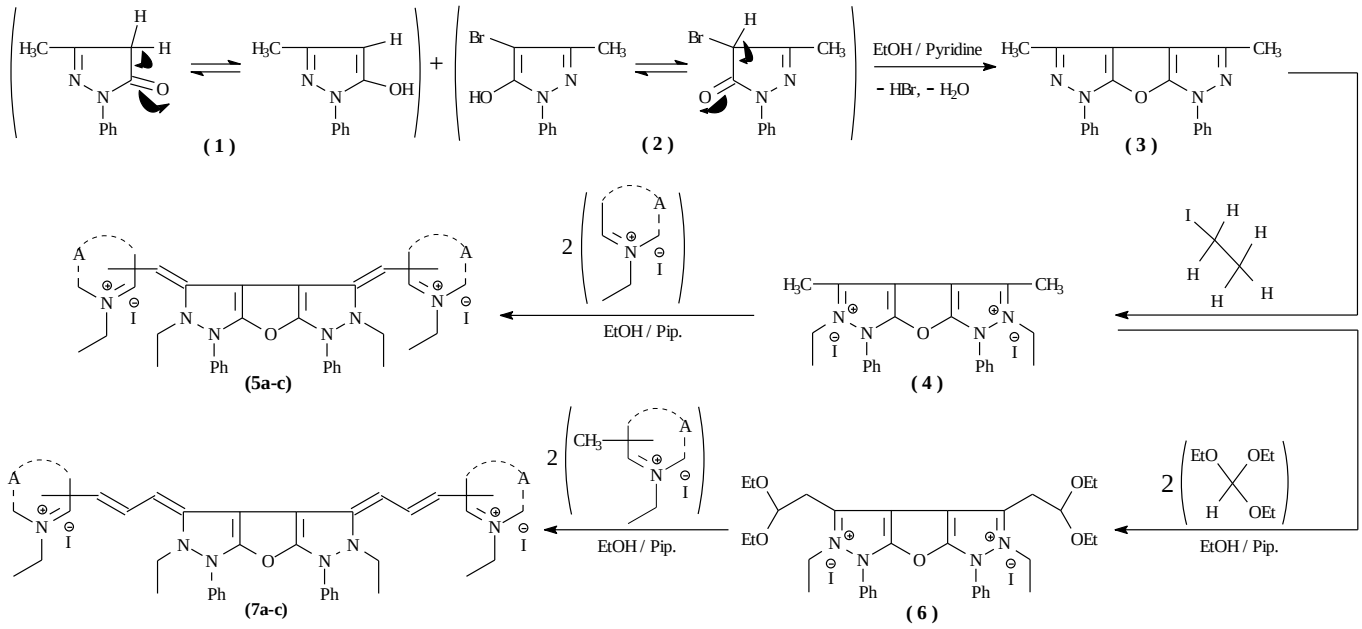

Scheme 1. Synthesis strategy of the prepared compounds

<u>Substitutes in Scheme (1)</u>:
(5a-c): A=1-ethyl pyridinium-4-yl salt (a); 1-ethyl quinolinium-4-yl salt (b); 2-ethyl isoquinolinium-1-yl salt (c).
(7a-c): A=1-ethyl pyridinium-2-yl salt (a); 1-ethyl quinolinium-2-yl salt (b); 1-ethyl pyridinium-4-yl salt (c).

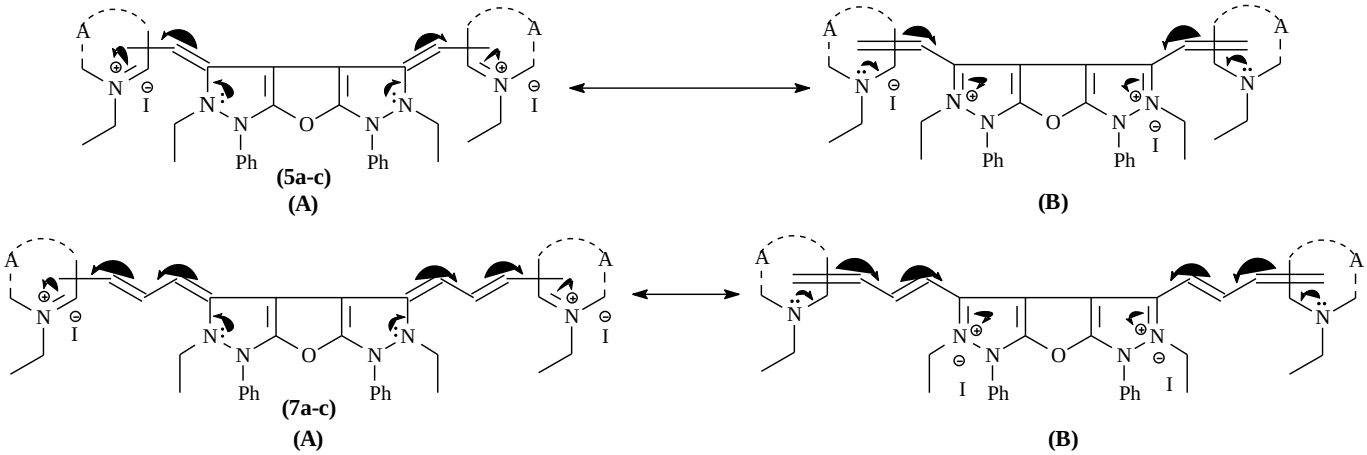

Scheme 2. Colour intensity illustration of the synthesized cyanine dyes (5a-c) and (7a-c)

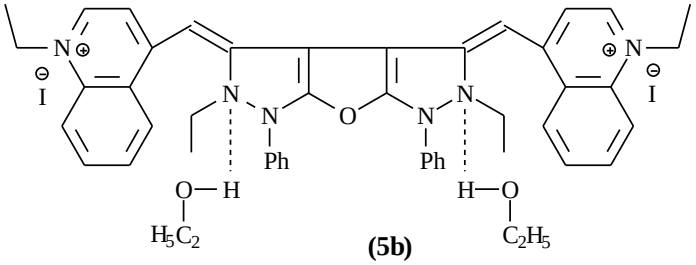

(5b)

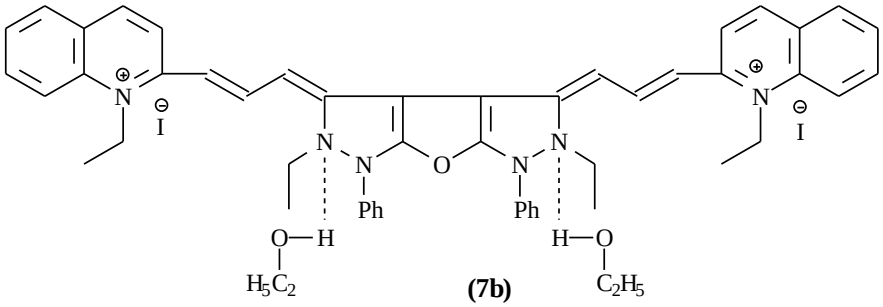

(7b)

Scheme (3) (A). Hydrogen bond formation between the cyanine dyes (5b), (7b) and ethanol molecules (specific solvent effect).

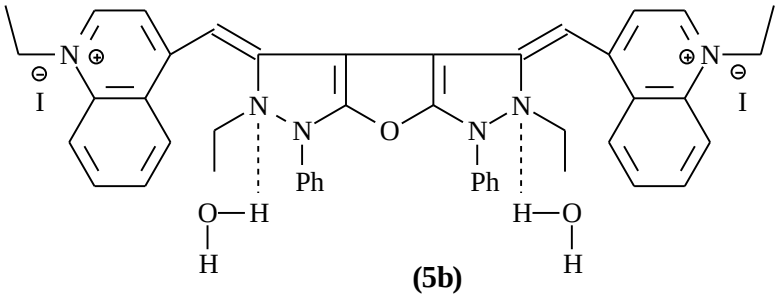

(5b)

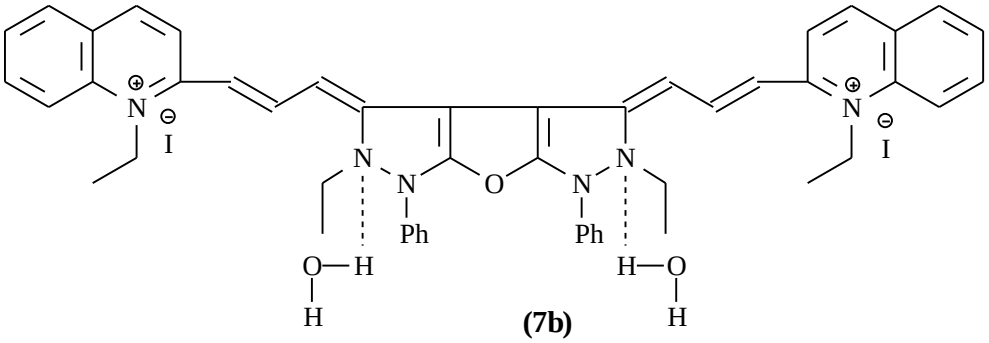

(7b)

Scheme (3) (B). Hydrogen bond formation between the cyanine dyes (5b), (7b) and water molecules (specific solvent effect)

Effects of pH media on the colour change of the cyanine dye (5b)

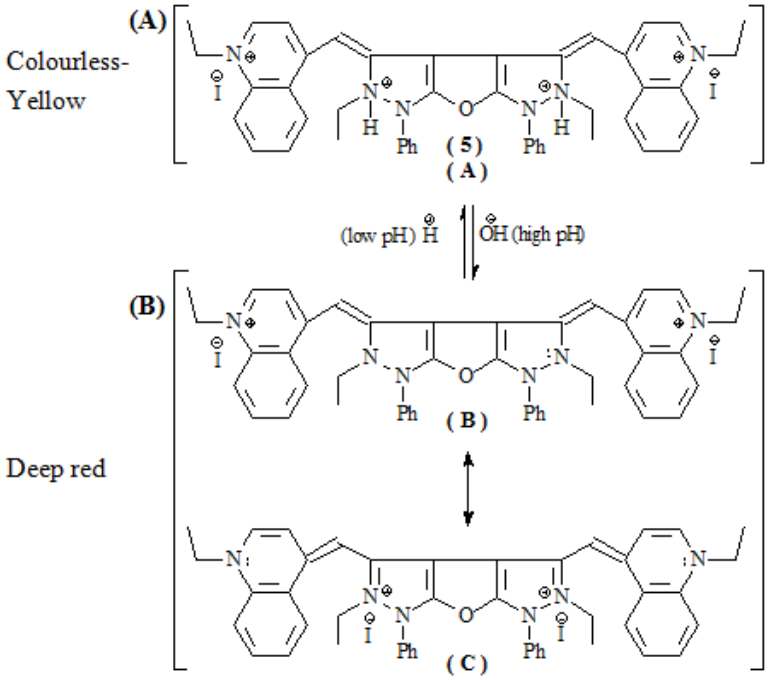

Scheme (4). Decolourization (protonation) and colourization (deprotonation) of the cyanine dye (5b) in acid and base media, respectively (acido-basic equilibrium).

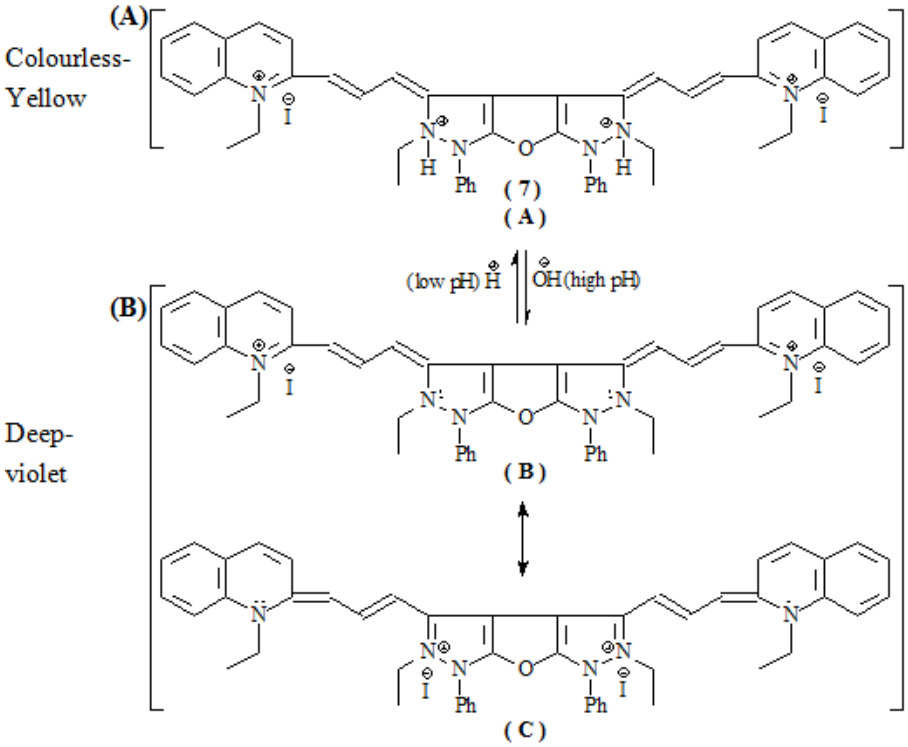

Scheme (4) Continue. Decolourization (protonation) and colourization (deprotonation) of the cyanine dye (7b) in acid and base media, respectively (acido-basic equilibrium)

Copyright © 2017 by Academic Publishing House Researcher s.r.o.

Published in the Slovak Republic
European Journal of Molecular Biotechnology
Has been issued since 2013.
ISSN: 2310-6255
E-ISSN: 2409-1332
2017, 5(1): 43-49

DOI: 10.13187/ejmb.2017.1.43
www.ejournal8.com

MEDT Study of the Mechanism and Regioselectivity of Diazocompounds and Alkenes in [3+2] Cycloaddition Reaction

A. Zeroual [a,b], M. El Idrissi [a], R. El Ajlaoui [d], N. Ourhriss [b], S. Abouricha [d], N. Mazoir [b,c], A. Benharref [b], A. El Hajbi [a]

[a] Laboratory of Physical Chemistry, Faculty of Science, Chouaïb Doukkali University, El Jadida, Morocco
[b] Laboratory of Biomolecular Chemistry, Natural Substances and Reactivity, URAC 16, Faculty of Sciences Semlalia, Cadi Ayyad University, Marrakech, Morocco
[c] Department of Chemistry, Faculty of Sciences El Jadida, Chouaib Doukkali University, El Jadida, Morocco
[d] Laboratory of Interdisciplinary Research in Science and Technology, Poly Disciplinary Faculty, Sultan Moulay Slimane University, Beni Mellal, Morocco

Abstract

The mechanism and regioselectivity of diazomethane with 2-methyl-but-2-ene and (diazomethylene)dibenzene with Methylene-trifluoromethyl-phosphane in [3+2] cycloaddition, have been theoretically studied at the DFT/ B3LYP/6-31(d) computational level. The possible ortho/meta regioselective channels were explored and characterized, the energies analysis associated with the different reaction pathways and the analysis of the density map of the transition indicates that the 1,3-DC reaction of diazomethane with 2-methyl-but-2-ene and (diazomethylene)dibenzene with Methylene-trifluoromethyl-phosphane are highly regioselective, in good agreement with the experimental observations.

Keywords: Molecular Electron Density Theory, chemoselective, regioselective, [3+2] cycloaddition, the potential electrostatic.

1. Introduction

The reaction of a 1,3-dipole to an double bond is a classic reaction in organic chemistry for the synthesis of five-membered rings. The [2+3] dipolar cycloaddition reactions are used for the preparation of molecules of importance for both biology and industry. These reactions are also used for the synthesis of natural products such as sugar derivatives, l-lactams, amino acids, alkaloids, and pharmacological products such as pyrazolines having several biological activities (anti-inflammatory, analgesic and herbicides) (El Sayed et al., 2012; Khode et al., 2009). Among the products prepared from the cycloaddition reactions are pyrazolines which possess important pharmacological and biological activities such as: antiviral (Rollas, S., Küçükgüzel, Ş. G., 2007), antimicrobial (Sahu et al., 2008; Samshuddin et al., 2012), anticancer (Bansal, Y., Silakari, O., 2012), antitumor (Chauhan et al., 2011) and these products as good derivatives as corrosion inhibitors for mild steel in hydrochloric acid medium (addouri et al., 2009; Cherrak et al., 2017). In 2008 a distortion/interaction (Osuna, Houk 2009; Ess, Houk, 2009) was introduce by Houk (Ess, Houk 2008) to explain the reactivity, this model is analogous of that proposed by Bicklehaupt in 1999 (Bickelhaupt 2014; Fernández, Bickelhaupt 2014). Houk found that the activation enthalpies correlated very nicely with distortion energies. The partition of the total density of the

TS geometry into two separated structure does not any physical sense within density functional DFT (Hohenberg, Kohn, 2014). Consequently, the energy of two Reagents cannot be correlated with the energy of TS because each of them losses the external potential created by the other Reagents. The changes in the electron density and not molecular orbital interaction are responsible for the reactivity in organic molecules (Domingo, 2014). Very recently Domingo proposed a new theory to study the reactivity in organic chemistry named Molecular Electron Density Theory (MEDT) (Domingo et al., 2016; Ríos-Gutiérrez et al., 2015).

Herein, in order to understand the molecular mechanism and the regioselectivity of the [2+3] dipolar cycloaddition reaction between diazomethane and alkenes 1-2 (scheme 1), a theoretical characterization of the molecular mechanism of these [2+3] dipolar cycloaddition reactions is carried out within the MEDT using DFT methods at the B3LYP/6-31G(d) computational level.

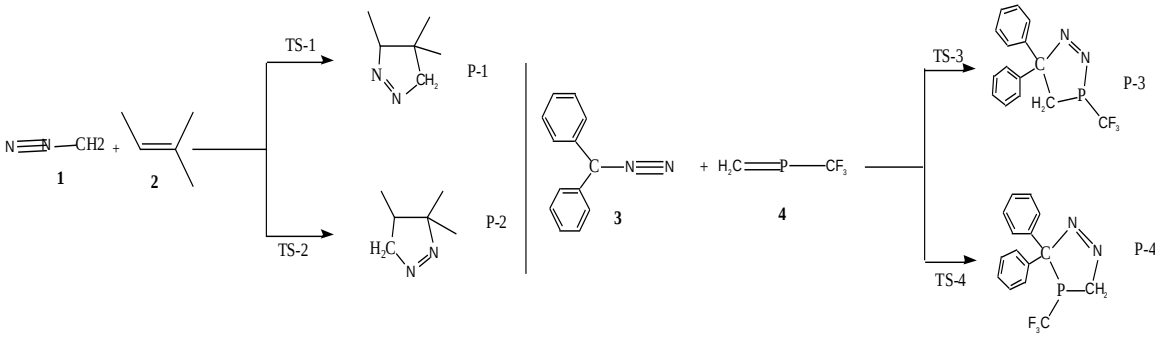

Scheme 1. Competitive regio-isomeric pathways associated with [2+3] cycloaddition reactions of the diazomethane (1) with 2-methyl-but-2-ene (2) and (diazomethylene)dibenzene (3) with Methylene-trifluoromethyl-phosphane (4).

2. Computational methods

DFT computations were carried out using the B3LYP functional (Yanai et al., 2004), together with the standard 6-31(d) basis set (Yanai et al., 1982). The optimizations have been realized using the Berny analytical gradient optimization method. All computations have been shown with the Gaussian 09 suite of programs (Frisch et al., 2009). The global electrophilicity index (Parr et al., 2009) ω, was given by the following expression $\omega = \frac{\mu^2}{2\eta}$, in terms of the electronic chemical potential μ and the chemical hardness η. Both quantities could be approached in terms of the one-electron energies of the frontier molecular orbital HOMO and LUMO, ε_H and ε_L as $\mu = \frac{\varepsilon_H + \varepsilon_L}{2}$ and $\eta = \varepsilon_H - \varepsilon_L$, respectively. The empirical nucleophilicity index N (Domingo et al., 2008; Domingo, Pérez, 2011), based on the HOMO energies obtained within the Kohn-Sham (Kohn, Sham, 1965), and defined as $N = E_{HOMO}(Nu) - E_{HOMO}(TCE)$. the nucleophilicity was referred to tetracyanoethylene (TCE). This choise allowed us to handle conveniently a nucleophilicity scale of positive values. Electrophylic P_k^+ and nucleophilic P_k^- Par functions were obtained through analysis of the Mulliken atomic spin density (ASD) of the radical anion and radical cation of the reagents. The local electrophilicity and the local nucleophilicity indices were evaluated using the following expressions $\omega_k = \omega P_k^+$ and $N_k = NP_k^-$ (Zeroual et al., 2015; El Idrissi et al., 2016; Zeroual et al., 2015; Ourhriss et al., 2017; Zoubir et al., 2017; Zeroual et al., 2015). The stationary points were characterized by frequency computations in order to verify that TSs have one and only one imaginary frequency. Intrinsic reaction coordinate (IRC) (Fukui, 1970) pathways were traced to verify the connectivity between minima and associated TSs. Solvent effets of dichloromethane were taken into account through single point energy calculation using the polarizable continuum model (PCM) developed by Tomasi's group in the framework of the self-consistent reaction field (Tomasi, Persico, 1994).

3. Results and discussion

This theoretical study has been divided into three parts: (1) first, an analysis of the DFT reactivity indices of the reagents involved in these cycloaddition reactions; (2) then, a PES study of the reactions involved in these cycloaddition reactions are discussed and characterized; (3) finally, an analysis of the transition state structures are analyzed.

3.1. DFT analysis based on the global and local reactivity indexes

In order to understand the mechanism of the cycloaddition reactions studied, we used DFT B3LYP/6-31G (d) to calculate the global indices shown in Table 1 the electronic chemical potential μ, chemical hardness η, global electrophilicity ω and nucleophilicity N of the diazomethane (1), 2-methyl-but-2-ene (2), (diazomethylene)dibenzene (3) and Methylene-trifluoromethyl-phosphane (4).

Table 1. Electronic chemical potential μ, chemical hardness η, electrophilicity ω and nucleophilicity N calculated using DFT B3LYP/6-31G (d) (eV)

System	μ	η	w	N
1	-3.64	4.72	1.40	3.52
2	-2.55	7.17	0.43	3.39
3	-3.35	3.70	1.52	4.32
4	-5.00	5.72	2.18	1.66

The electronic chemical potential of 2-methyl-but-2-ene 2, μ = −2.55 eV, is higher than that of diazomethane 1, μ = −3.64 eV, thereby indicating that along a polar reaction the global electron density transfer (GEDT) will go from 2-methyl-but-2-ene 2 towards diazomethane 1. In the reaction 2 the electronic chemical potential of the (diazomethylene)dibenzene (3), μ = −3.35 eV, is higher than that of methylene-trifluoromethyl-phosphane (4), μ = −5.00 eV, thereby indicating that along a polar reaction the GEDT will go from (diazomethylene)dibenzene (3) to methylene-trifluoromethyl-phosphane (4).

The diazomethane (1) presents an electrophilicy ω index of 1.40 eV and a nucleophilicity N index of 3.52 eV, being classified as strong electrophile than ω index of the 2-methyl-but-2-ene (2), 0.43 eV and a nucleophilicity N index of 3.39 eV. Consequently, the diazomethane 1 is classified as a strong electrophile, while the -methyl-but-2-ene (2) a strong nucleophile. On the other hand, the electrophilicity ω and nucleophilicity N indices of the (diazomethylene)dibenzene (3) are 1.52 and 4.32 eV, being classified on the borderline of marginal electrophiles and as a strong nucleophile. Inclusion of one florine atom of the carbon atom of (diazomethylene)dibenzene (3) notably increases both the electrophilicity ω and nucleophilicity N index of trifluoromethyl-phosphane (4) to 2.18 and 1.66 eV, being classified as a moderate nucleophile and a strong electrophile. Consequently, the trifluoromethyl-phosphane (4) will participate as electrophile and the (diazomethylene)dibenzene (3) will participate as nucleophile.

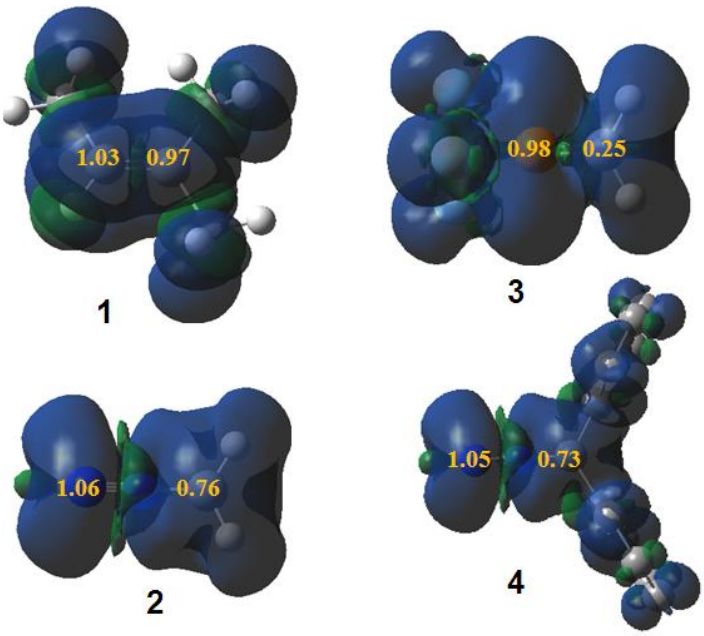

Fig. 1. Map of the ASD of the neutral radical Po of the diazomethane (1), 2-methyl-but-2-ene (2), (diazomethylene)dibenzene (3) and Methylene-trifluoromethyl-phosphane (4).

The deference between an electrophilicy of the reagents is smaller than one indicating that these reactions are not polar reactions the fact that we use atomic spin density of the neutral radical P0, from Figure 2 we can observed that P0 of the carbon atom C3 is 1.03 and C2 is 0.97, for the diazomethane P0 of the nitrogen atom strong is 1.06 and for the carbon atom is 0.76, this result indicating that the best interaction will be between C3 and N1 and C2 with carbon of diazomethane in good agreement with experimental observations.

3.2 Energies study

Due to the non-symmetry of both reagents, [2+3] cycloaddition reactions of the diazomethane (1) with 2-methyl-but-2-ene (2) and (diazomethylene)dibenzene (3) with Methylene-trifluoromethyl-phosphane (4) can take place through two competitive reactive channels namely meta and ortho (scheme 1) and to interpret the regioselectivity experimentally observed in these reactions, the energies and relative energies were calculated and summarized in table 2, PES of the reaction was calculated by B3LYP/6-31G(d) method. Intrinsic Reaction Coordinate (IRC) calculations were performed to characterize the transition states on the PES (Figure 2).

Table 2. B3LYP/6-31G (d) energies E (in a.u.) and relative energies (ΔE, in kcal/mol) of the reagents, transition states and products.

System	E	ΔE
1+2	-345.28284	-------
TS1	-345.24892	21.28
TS 2	-345.24605	23.08
P 1	-345.33060	-29.97
P 2	-345.32837	-28.57
3+4	-1329.10559	---------
TS3	-1329.05759	30.12
TS 4	-1329.05579	31.25
P 3	-1329.14676	-25.83
P4	-1329.14086	-22.13

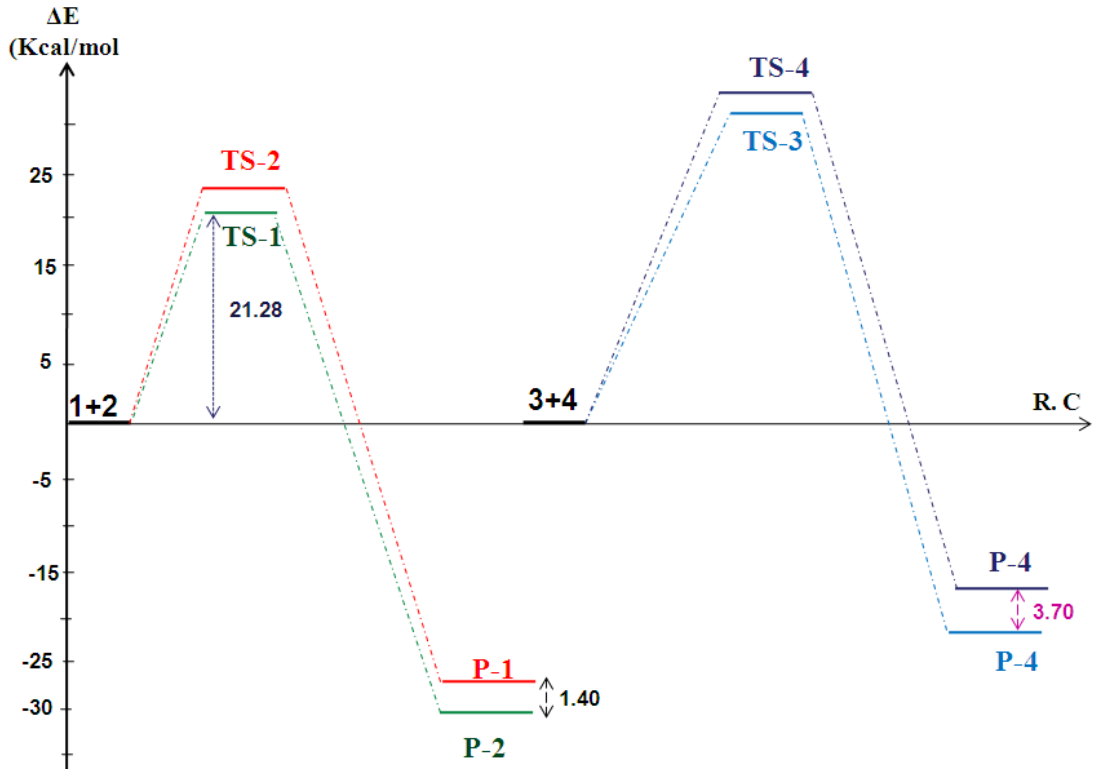

Fig. 2. Pathways for [2+3] cycloaddition reactions of the diazomethane (1) with 2-methyl-but-2-ene (2) and (diazomethylene)dibenzene (3) with methylene-trifluoromethyl-phosphane (4)

The activation energies of reactions of the diazomethane (1) with 2-methyl-but-2-ene (2) and (diazomethylene)dibenzene (3) with methylene-trifluoromethyl-phosphane (4) associated with the two competitive reactive channels are 21.28 (TS-1m), 23.08 (TS-1o), 30.12 (TS-2m) and 31.25 (TS-2o) kcal mol−1 these value indicate that the most favorable channel is meta. In these 32CA reaction, the formation of the products 1-m and 2-m are strongly exothermic by 29.97 and 25.83 kcal mol−1 respectively, the formation of the products 1-o and 2-o are exothermic by 28.57 and 22.13 respectively. Analysis of these relative energies leads to some appealing conclusions: (1) this 32CA reaction the formation of the 1-m and 2-m are kinetically favored (2) the strong exothermic character of this 32CA reaction makes the formation of the products 1m, 1o, 2m and 2o are irreversible Consequently, formation of the product 1m and 2-m are under kinetic and thermodynamic control, These results are in agreement with the meta regioselectivity experimentally observed.

3.3. Geometries study

The geometries of the TSs involved in the two competitive reaction channels are given in Fig. 3. At the meta TSs, the lengths of the N1–C3 and C2–C forming bonds are 1.978 and 2.401 Å (TS-1) and , the lengths of the P–N1 and C–C forming bonds are 2.260 and 2.133 Å (TS-3), while at the ortho TSs, the lengths of the C3–C and C2–N1 forming bonds are 2.231 and 2.113Å (TS-2), the lengths of the P–C and N1–C forming bonds are 2.826 and 2.517 Å (TS-4). Some appealing conclusions can be drawn from these geometrical parameters: (1) the TSs associated with the meta channels are more asynchronous than those associated with the ortho one. On other hand the density map of the transition of the transition state indicating that the formation of the products 2-o and 2-o not favored, because the density map are separate, in contrary in TS-1o and TS-2o the density map not separate which indicates that formation of the products 1-m and 2-m are favored.

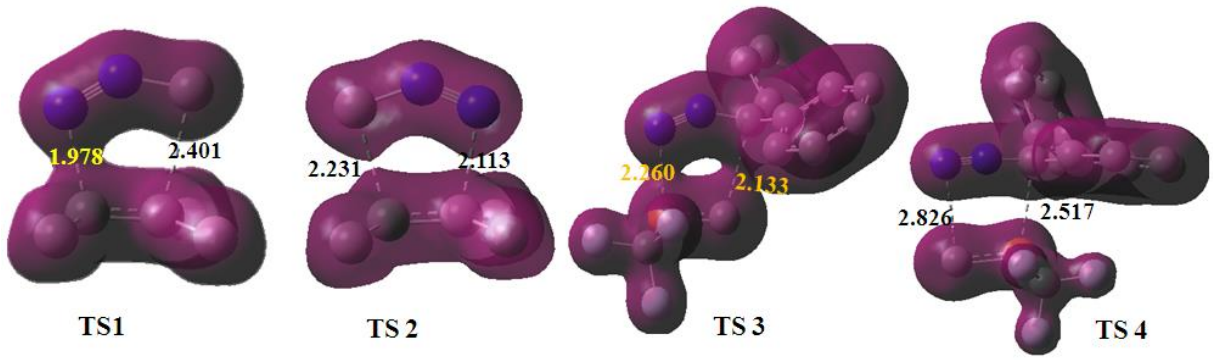

Fig. 3. DFT/6-31G(d) optimized density map and structures of the TSs of the [2+3] cycloaddition reactions of the diazomethane (1) with 2-methyl-but-2-ene (2) and (diazomethylene)dibenzene (3) with methylene-trifluoromethyl-phosphane (4). Lengths are given in Angstroms.

4. Conclusion

The mechanism and the regioselectivity of the [2+3] cycloaddition reactions of the diazomethane (1) with 2-methyl-but-2-ene (2) and (diazomethylene)dibenzene (3) with methylene-trifluoromethyl-phosphane (4) were studied using DFT B3LYP/6-31G (d).

The theoretical results obtained enabled us to conclude that:

the formation of the products 2-o and 2-o not favored, because the density map are separate, in contrary in TS-1o and TS-2o the density map not separate which indicates that formation of the products 1-m and 2-m are favored.

The formation of the product 1m and 2-m are under kinetic and thermodynamic control, in agreement with the meta regioselectivity experimentally observed.

Map of the ASD of the neutral radical P0 of the reagents, indicating that the best interaction will be between C3 and N1 and C2 with carbon of diazomethane in good agreement with experimental observations.

References

Addouri et al., 2009 – *Addouri, Y., Takfaoui, A., Abrigach, F., El Azzouzi, M., Zarrouk, A., El-Hajjaji, F., Touzani, R., Sdassi, H.* (2017). Tridentate Pyrazole Ligands: Synthesis, Characterization and Corrosion Inhibition properties with Theoretical investigations. *Journal of Materials and Environmental Sciences*, 8 (3): 845-856.

Bansal, Silakari, 2012 – *Bansal, Y., Silakari, O.* (2012). The therapeutic journey of benzimidazoles: a review, *Bioorganic & Medicinal Chemistry,* 20: 6208–6236.

Bickelhaupt, 2014 – *Bickelhaupt F. M.* (2014). Understanding reactivity with Kohn–Sham molecular orbital theory: E2–SN2 mechanistic spectrum and other concepts. *J Comput Chem,* 20: 114–128.

Chauhan et al., 2011 – *Chauhan, A., Sharma, P. K., Kaushik, N.* (2011). Pyrazole: A Versatile Moiety. *International Journal of Chem Tech Research,* 3: 11-17.

Cherrak et al., 2017– *Cherrak, K., Dafali, A., Elyoussfi, A., El Ouadi, Y., Sebbar, N. K., El Azzouzi, M., Elmsellem, H., Essassi, E. M., Zarrouk, A.* (2017). Two new benzothiazine derivatives as corrosion inhibitors for mild steel in hydrochloric acid medium. *Journal of Materials and Environmental Sciences,* 8 (2): 636-647.

Domingo et al., 2008 – *Domingo, L. R., Chamorro, E., Pérez, P.* (2008). Understanding the Reactivity of Captodative Ethylenes in Polar Cycloaddition Reactions. A Theoretical Study, *J. Org. Chem*, 73: 4615-4624.

Domingo, 2014 – *Domingo, L. R.* (2014). A new C–C bond formation model based on the quantum chemical topology of electron density. RSC Adv, 4: 32415–32428.

Domingo et al., 2016 – *Domingo, L R., Ríos-Gutiérrez, M., Pérez, P.* (2016). A new model for C–C bond formation processes derived from the Molecular Electron Density Theory in the study of the mechanism of [3+2] cycloaddition reactions of carbenoid nitrile ylides with electron-deficient ethylenes. *Tetrahedron,* 72: 1524–1532.

Domingo, Pérez, 2011 – *Domingo, L. R., Pérez, P.* (2011). The nucleophilicity N index in organic chemistry, *Org. Biomol. Chem*, 9: 7168-7175.

El Idrissi et al., 2016 – *El Idrissi, M., El Haib, A., Zoubir, M., Hammal, R., Zeroual, A., EL Hajbi, A.* (2016). Understanding the regioselectivite of the Baeyer-Villiger reaction of bicyclo[4.2.0]octan-7-one and bicyclo[3.2.0]heptan-6-one: A DFT Study, *Journal of Computational Methods in Molecular Design,* 6: 75-79.

El-Sayed et al., 2012 – *El-Sayed, M. A.-A., Abdel-Aziz, N. I., Abdel-Aziz, A. A.-M., El-Azab, A.S., ElTahir, K. E.H.* (2012). Synthesis, biological evaluation and molecular modeling study of pyrazole and pyrazoline derivatives as selective COX-2 inhibitors and anti-inflammatory agents. Part 2, *Bioorganic & Medicinal Chemistry,* 20: 3306–3316.

Ess, Houk, 2008 – *Ess, D. H., Houk, K. N.* (2008). Theory of 1, 3-dipolar cycloadditions: distortion/interaction and frontier molecular orbital models, *J Am Chem Soc,* 130: 10187–10198.

Ess, Houk, 2009 – *Ess, D. H., Houk, K. N.* (2009). Theory of 1, 3-dipolar cycloadditions: distortion/interaction and frontier molecular orbital models: Cycloaddition Reactions of Butadiene and 1,3-Dipoles to Curved Arenes, Fullerenes, and Nanotubes: Theoretical Evaluation of the Role of Distortion Energies on Activation Barriers, *Chemistry – A European Journal,* 15: 12905–13267.

Fernández, Bickelhaupt, 2014 – *Fernández, I., Bickelhaupt, F.M.* (2014). The activation strain model and molecular orbital theory: understanding and designing chemical reactions, *Chemical Society Reviews*, 43: 4906-4908.

Frisch et al., 2009 – Gaussian 09, Revision A.02, Frisch M. J. et al.

Fukui, 1970 – *Fukui, K.* (1970). Formulation of the reaction coordinate, *J. Phys. Chem*, 74: 4161–4163.

Hohenberg, Kohn 2014 – *Hohenberg, P., Kohn, W.* (1964). Inhomogeneous Electron Gas. *Phys Rev B,* 136: 864–871.

Khode et al., 2009 – *Khode, S., Maddi, V., Aragade, P., Palkar, M., Ronad, P. K., Mamledesai, S., Thippeswamy, A.H.M., Satyanarayana, D.* (2009). Synthesis and pharmacological evaluation of a novel series of 5-(substituted)aryl-3-(3-coumarinyl)-1-phenyl-2-pyrazolines as novel anti-inflammatory and analgesic agents. *European Journal of Medicinal Chemistry,* 44: 1682–1688.

Kohn, Sham, 1965 – *Kohn, W., Sham, L.* (1965). Self-Consistent Equations Including Exchange and Correlation Effects, *J. Phys. Rev A*, 140: 1133-1138.

Osuna, Houk, 2009 – *Osuna, S., Houk, K.N.* (2009). Cycloaddition Reactions of Butadiene and 1,3-Dipoles to Curved Arenes, Fullerenes, and Nanotubes: Theoretical Evaluation of the Role of Distortion Energies on Activation Barriers. *Chem Eur J,* 15: 13219–13231.

Ourhriss et al., 2017 – *Ourhriss, N., Zeroual, A., Ait Elhad, M., Mazoir, N., Abourriche, A., Gadhi, C. A., Benharref, A., El Hajbi, A.* (2017). Synthesis of 1-isopropyl-4,7-dimethyl-3-nitronaphthalene: An experimental and theoretical study of regiospecific nitration, *Journal of Materials and Environmental Sciences,* 8 (4): 1385-1390.

Parr et al., 2009 – *Parr, R. G., Szentpaly, L. V., Liu, S.* (1999). Electrophilicity Index, *J Am ChemSoc,* 121: 1922-1924.

Ríos-Gutiérrez et al., 2015 – *Ríos-Gutiérrez, M., Pérez, P., Domingo, L. R.* (2015). A molecular electron density theory study of the [3 + 2] cycloaddition reaction of nitrones with ketenes, *RSC Adv,* 5: 58464-58477.

Rollas, Küçükgüzel, 2007 – *Rollas, S., Küçükgüzel, Ş. G.* (2007). Biological Activities of Hydrazone Derivatives. *Molecules,* 12: 1910-1939.

Sahu et al, 2008– *Sahu, S. K., Banerjee, M., Samantray, A., Behera, C., Azam, M. A.* (2008). Synthesis, Analgesic, Anti-inflammatory and Antimicrobial Activities of Some Novel Pyrazoline Derivatives. *Tropical Journal of Pharmaceutical Research,* 7: 961-968.

Samshuddin et al., 2012 – *Samshuddin, S., Narayana, B., Sarojini, B. K. Hassan Khan, M. T., Yathirajan, H. S., Darshan Raj C. G., Raghavendra, R.* (2012). Antimicrobial, analgesic, DPPH scavenging activities and molecular docking study of some 1,3,5-triaryl-2-pyrazolines. *Med Chem Res,* 21: 2012–2022.

Tomasi, Persico, 1994 – *Tomasi, J., Persico M.* (1994). Molecular Interactions in Solution: An Overview of Methods Based on Continuous Distributions of the Solvent, *Chem. Rev.*, 94: 2027–2094.

Yanai et al., 1982 – *Francl, M. M., Pietro, W. J., Hehre W. J.* (1982). A polarization-type basis set for second-row elements, *J. Chem. Phys,* 77: 3654-3665.

Yanai et al., 2004 – *Yanai, T., Tew, D. P., Handy, N. C.* (2004). A new hybrid exchange? correlation functional using the Coulomb-attenuating method (CAM-B3LYP) *Chemical Physics Letters,* 393: 51–57.

Zeroual et al., 2015 – *Zeroual, A., Benharref, A., El Hajbi, A.* (2015). Theoretical study of stereoselectivity of the [1+2] cycloaddition reaction between (1S,3R,8S)-2,2-dichloro-3,7,7,10-tetramethyltricyclo[6,4,0,01.3]dodec-9-ene and dibromocarbene using density functional theory (DFT) B3LYP/6-31G*(d), *J Mol Model,* 21: 2594-2599.

Zeroual et al., 2015 – *Zeroual, A., El Haib, A., Benharref, A., El Hajbi A.* (2015). A combined experimental and theoretical study of highly chemioselectivity acetylation of diterpene, *Journal of Computational Methods in Molecular Design,* 5: 58-62.

Zeroual et al., 2015 – *Zeroual, A., Zoubir, M., Hammal, R., Benharref, A., El Hajbi, A.* (2015). Understanding the regioselectivity and reactivity of Friedel–Crafts benzoylation using Parr functions, Mor. J. Chem, 3: 356-360.

Zoubir et al., 2017 – *Zoubir, M., Zeroual, A., El Idrissi, M., Bkiri, F., Benharref, A., Mazoir, N., El Hajbi A.* (2017). Experimental and theoretical analysis of the reactivity and regioselectivity in esterification reactions of diterpenes (totaradiol, totaratriol, hinikione and totarolone), *Mediterranean Journal of Chemistry,* 6(4): 98-107.